

5-1-2021

A comprehensive review of retinal vascular and optical nerve diseases based on optical coherence tomography angiography

Fatma Taher
Zayed University

Heba Kandil
University of Louisville

Hatem Mahmoud
Al-Azhar University

Ali Mahmoud
University of Louisville

Ahmed Shalaby
University of Louisville

See next page for additional authors

Follow this and additional works at: <https://zuscholars.zu.ac.ae/works>



Part of the [Computer Sciences Commons](#), and the [Medicine and Health Sciences Commons](#)

Recommended Citation

Taher, Fatma; Kandil, Heba; Mahmoud, Hatem; Mahmoud, Ali; Shalaby, Ahmed; Ghazal, Mohammed; Alhalabi, Marah Talal; Sandhu, Harpal Singh; and El-Baz, Ayman, "A comprehensive review of retinal vascular and optical nerve diseases based on optical coherence tomography angiography" (2021). *All Works*. 4206.

<https://zuscholars.zu.ac.ae/works/4206>


This Article is brought to you for free and open access by ZU Scholars. It has been accepted for inclusion in All Works by an authorized administrator of ZU Scholars. For more information, please contact scholars@zu.ac.ae.

Author First name, Last name, Institution

Fatma Taher, Heba Kandil, Hatem Mahmoud, Ali Mahmoud, Ahmed Shalaby, Mohammed Ghazal, Marah Talal Alhalabi, Harpal Singh Sandhu, and Ayman El-Baz

Article

A Comprehensive Review of Retinal Vascular and Optical Nerve Diseases Based on Optical Coherence Tomography Angiography

Fatma Taher ^{1,†} , Heba Kandil ^{2,†} , Hatem Mahmoud ³, Ali Mahmoud ² , Ahmed Shalaby ² , Mohammed Ghazal ⁴ , Marah Talal Alhalabi ⁴ , Harpal Singh Sandhu ⁵ and Ayman El-Baz ^{2,*} 

- ¹ The College of Technological Innovation, Zayed University, Dubai 19282, United Arab Emirates; fatma.taher@zu.ac.ae
 - ² Bioengineering Department, University of Louisville, Louisville, KY 40292, USA; hekand01@louisville.edu (H.K.); ahmahm01@louisville.edu (A.M.); ahmed.shalaby@louisville.edu (A.S.)
 - ³ Ophthalmology Department, Faculty of Medicine, Al-Azhar University, Cairo 11651, Egypt; hatem.samy@hotmail.com
 - ⁴ Electrical and Computer Engineering Department, Abu Dhabi University, Abu Dhabi 59911, United Arab Emirates; mohammed.ghazal@adu.ac.ae (M.G.); marah.alhalabi@adu.ac.ae (M.T.A.)
 - ⁵ Ophthalmology Department, School of Medicine, University of Louisville, Louisville, KY 40292, USA; harpal.sandhu@gmail.com
- * Correspondence: aselba01@louisville.edu
† These authors shared the first-authorship.



Citation: Taher, F.; Kandil, H.; Mahmoud, H.; Mahmoud, A.; Shalaby, A.; Ghazal, M.; Alhalabi, M.T.; Sandhu, H.S.; El-Baz, A. A Comprehensive Review of Retinal Vascular and Optical Nerve Diseases Based on Optical Coherence Tomography Angiography. *Appl. Sci.* **2021**, *11*, 4158. <https://doi.org/10.3390/app11094158>

Academic Editors: Jim Tang and Sos Agaian

Received: 17 March 2021
Accepted: 28 April 2021
Published: 1 May 2021

Publisher's Note: MDPI stays neutral with regard to jurisdictional claims in published maps and institutional affiliations.



Copyright: © 2021 by the authors. Licensee MDPI, Basel, Switzerland. This article is an open access article distributed under the terms and conditions of the Creative Commons Attribution (CC BY) license (<https://creativecommons.org/licenses/by/4.0/>).

Abstract: The optical coherence tomography angiography (OCTA) is a noninvasive imaging technology which aims at imaging blood vessels in retina by studying decorrelation signals between multiple sequential OCT B-scans captured in the same cross section. Obtaining various vascular plexuses including deep and superficial choriocapillaris, is possible, which helps in understanding the ischemic processes that affect different retina layers. OCTA is a safe imaging modality that does not use dye. OCTA is also fast as it can capture high-resolution images in just seconds. Additionally, it is used in the assessment of structure and blood flow. OCTA provides anatomic details in addition to the vascular flow data. These details are important in understanding the tissue perfusion, specifically, in the absence of apparent morphological change. Using these anatomical details along with perfusion data, OCTA could be used in predicting several ophthalmic diseases. In this paper, we review the OCTA techniques and their ability to detect and diagnose several retinal vascular and optical nerve diseases, such as diabetic retinopathy (DR), anterior ischemic optic neuropathy (AION), age-related macular degeneration (AMD), glaucoma, retinal artery occlusion and retinal vein occlusion. Then, we discuss the main features and disadvantages of using OCTA as a retinal imaging method.

Keywords: optical nerve diseases; OCTA; retinal; vascular diseases

1. Introduction

Optical coherence tomography angiography (OCTA) is a novel imaging modality that noninvasively and rapidly images the retinal microvasculature in multiple layers with a resolution resembling histologic appearance [1,2]. It can identify retinal vessels by the detection of intensity and/or phase property variations of optical coherence tomography (OCT) signals in multiple B-scans at the same point resulting from red blood cell movement [3]. OCTA generates angiographic images by employing motion contrast imaging to obtain high-resolution volumetric blood flow information with excellent intra-visit repeatability [4].

OCTA employs an algorithm called the split spectrum amplitude decorrelation angiography (SSADA), which detects the flow of blood in the retinal microvasculature with no use of dye [5]. SSADA allows for obtaining OCTAs of high quality using the same available speeds in a retinal commercial OCT system [6]. An advantage of using SSADA is that it enhances the flow detection's signal-to-noise ratio [7]. Normal OCT provides in-depth imaging of the retinal and choroidal vasculature. The retina consists of a three-neuron circuit that detects light and then transmits that signal to the brain via the optic nerve. The photoreceptors are located in the outer retina, which is avascular. Thus, OCTA images of the outer retina show no vessels under normal conditions. The outer retina receives its oxygen from the choriocapillaris, the richly vascular layer of the eye as deep as the retinal pigment epithelium (RPE), which is a monolayer of cells that divides the outer retina from the choroid. OCTA readily images both the choroid and choriocapillaris. After detecting light, photoreceptor cells transmit their electrical signal to bipolar cells in the middle retina, which in turn connect to retinal ganglion cells in the inner retina. These funnel into the optic nerve, which travels posteriorly through the optic chiasm to the brain. Oxygen to the middle and inner retina is supplied by the deep and superficial plexuses of the retinal vasculature, both of which are beautifully imaged by OCTA. Finally, there is a peripapillary vasculature supplied by the central retinal artery that encircles the optic nerve and supplies the pre-laminar optic nerve. Thus, under normal conditions, OCTA provides high-resolution imaging of vessels in the choroid, choriocapillaris, middle and inner retina, and peripapillary vessels.

Thanks to OCTA, retinal, choroidal and optic nerve vasculature can be studied safely with no dye injection. Specific layers of the retina and choroid can be separately visualized by en-face OCTA which helps in detecting vascular changes level in the choriocapillaris, the middle choroid, the inner retina, and the outer retina [6]. It can demonstrate vessel density (VD), shape of the foveal avascular zone (FAZ), and alteration in retinal blood flow [8]. OCTA acquisition time is short compared to indocyanine green angiography (ICGA) or fluorescein angiography (FA) because there is no dependence on the dye's flooding kinetics. Instead, acquisition time depends on parameters such as scan volume, speed of eye tracking system, scan speed, resolution, and numbers of scans averaged [9].

OCTA's ability to detect the shape and morphology of FAZ is very helpful as FAZ is an indicator of the perifoveal microcirculation [10]. Important retinovascular diseases, such as retinal vein occlusion (RVO) and Diabetic Retinopathy (DR), interfere with the retinal microvascular circulation and alter FAZ size and shape [11]. OCTA can detect capillary dropout in DR better than FA because of lack of leakage [12].

In the following sections, we will discuss the advantages of OCTA as a new imaging modality in comparison with other modalities such as FA and ICGA. We will also provide a short review of clinical findings of OCTA in several retinal and optic-nerve-related diseases. The review aims to guide researchers regarding the capabilities of OCTA over current technologies in diagnosing ophthalmic diseases, which gives it a significant translational value.

OCTA Versus FA and ICGA

FA and ICGA are important diagnostic imaging techniques for evaluating multiple retinal diseases, in particular ones of vascular or inflammatory origin. These invasive tests use intravenous dye followed by multiple photographs over at least (10 to 30) min. They provide 2-D images with dynamic visualization of blood flow and a wide field of view [13,14]. Their images can be interpreted depending on the dye leakage, pooling, and staining patterns. While color fundus photography, FA, and ICG are generally presented as 2D images, there historically have been modalities for generating some degree of depth to these images. Scanning laser ophthalmoscopy (SLO) is an imaging modality based on a form of confocal microscopy [15]. It suffered in the past from an inability to represent true color, but improvements in this regard have been made. More recently, SLO has been combined with adaptive optics imaging techniques [16]. Despite some notable ad-

vantages to SLO, the technology is not ubiquitous in most ophthalmology clinics, and most commercial FA and ICG machines present 2D images.

Several studies in the literature have investigated using FA imaging modality diagnosing the posterior segment of the eye [17]. Despite that, FA has some limitations such as its inability to visualize different levels of major capillary networks separately. This is because FA is unable to differentiate deep capillary plexus (DCP) from superficial capillary plexus (SCP). Additionally, it is hard to use FA in obtaining enhanced images of perifoveal capillaries because it has a challenge in focusing images in case of macular edema existence [18]. Moreover, FA is an invasive, time-consuming and relatively expensive modality, which makes it not ideal for regular use in clinical settings. Fluorescein dye is known to be safe; however, its side effects include nausea, allergic reactions and anaphylaxis in some rare cases [6].

OCTA is a technique that is used to acquire angiographic information non-invasively without the need to use dye [17]. OCTA can capture images rapidly and check if the acquired images are of sufficient quality. If the acquired images are of low quality, OCTA can repeat the capturing process until images of good quality are obtained. FA in contrast has a time frame that is limited to capturing the capillary net images that are optimal. Individual vascular plexuses with the segmentation of the choriocapillaris, the middle choroid, the inner retina, and the outer retina can be visualized in the acquired en-face images [6]. OCTA outperforms FA in detection of macular ischemia because there is no dye leakage [19]. While FA cannot visualize DCP, OCTA is able to accurately delineate microvascular changes and ischemia in both DCP and SCP [1]. This is because OCTA does not have dye leakage and tissue staining problems, in addition to the longer wavelengths used in OCTA that can better penetrate through intraretinal hemorrhage [20]. Furthermore, OCTA is able to detect neovascularization elsewhere (NVE) while providing better visibility of new vessels than that produced by FA [21]. However, while NVE in the posterior pole can be readily imaged with OCTA, it suffers from the drawback that it does not image the periphery where a significant amount of NVE occurs.

2. Retinal Vascular Diseases

2.1. Diabetic Retinopathy (DR)

In 2015, there were about 415 million people diagnosed with diabetes mellitus worldwide [22]. Microvascular complications are the most common causes of diabetic patients' morbidity and mortality [23]. DR is an early clinical sign of microvascular complications in diabetes mellitus [24]. In developed countries, DR is considered a primary blindness cause among working-age adults [25].

DR has earlier signs which include tortuosity progression, caliber changes in arterioles and venules, and alterations in FAZ shape and size [26]. In addition, it is recognized by blood-retinal barrier breakdown, microaneurysm formation and pericyte loss. Another significant early event of DR is capillary nonperfusion which leads to tissue damage and ischemia over time [27]. OCTA offers the advantage of quantification of early features of DR particularly changes of vessel density in the macula and changes in FAZ area [28].

FA has been used to study foveal microvasculature and was able to show capillary dropout areas in DR; however, detection of the capillary alterations was limited by the capillary networks and the leakage superposition [29]. The OCTA provides a 3-D non-invasive vascular mapping of macular perfusion [30] while separating DCP and SCP; meanwhile, FA can barely show the DCP [6]. OCTA have shown that microvascular changes in DR are not confined to the SCP [31]. On the contrary, parafoveal-capillary dropout occur initially at the level of the DCP [32]. There are many obvious alternations, which can be detected in the OCTA scans due to the developing of DR. In the following subsection, these changes are discussed in detail.

2.1.1. Detection of DR

FAZ Enlargement

Size and morphology of the FAZ is an important indicator of capillary perfusion status within the macula; it correlates with the grade of DR, and abnormalities of FAZ can sometimes indicate macular ischemia [33].

One of the various clinical applications of OCTA in DR is its ability to evaluate the shape and the size of the FAZ area. Several clinical studies (Takase et al. [34], Suzuki et al. [35], Dupas et al. [36], Freiberg et al. [37], Eladawi et al. [38], Sahndu et al. [39]) reported enlargement of FAZ in diabetic patients versus normal healthy controls. Figure 1 shows enlargement of FAZ in DCP and SCP in a diabetic patient versus a normal control.

Takase et al. [34] found an enlargement of FAZ in the SCP in the healthy controls compared to eyes of patients of diabetic with DR and enlargement of FAZ in the DCP in the healthy controls compared to the eyes of diabetic patients with DR. Salz et al. [20] found an enlargement of FAZ in the SCP in the healthy controls compared to the eyes of diabetic patients with DR.

Suzuki et al. [35] also found an enlargement of FAZ in the SCP in the healthy controls compared to the eyes of diabetic patients with DR and enlargement of FAZ in the DCP in healthy controls compared to the eyes of diabetic patients with DR. They concluded that the enlargement of the FAZ is statistically significant in the DCP at a rate of 5.1% per year. There was also enlargement of FAZ in the SCP, but it was not statistically significant.

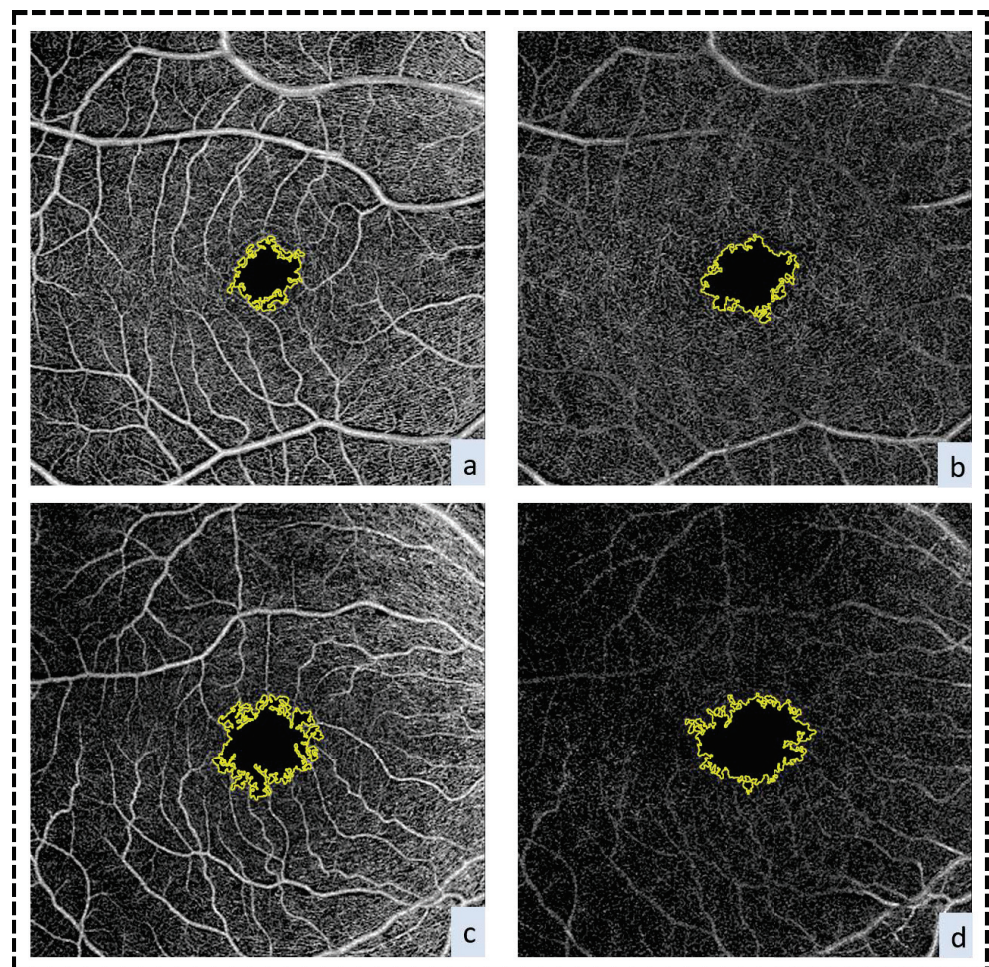


Figure 1. FAZ enlargement. (a) SCP for a normal subject, (b) DCP for a normal subject, (c) SCP for a diabetic patient, and (d) DCP for a diabetic patient.

Dupas et al. [36] found significant enlargement of FAZ in the SCP in the healthy controls compared to the eyes of diabetic patients with DR and normal visual acuity (VA). They found further enlargement of FAZ in the diabetic patients with DR and reduced VA. They concluded that the enlargement of FAZ in diabetic patients with DR is negatively correlated with VA.

Freiberg et al. [37] found enlargement of the mean horizontal FAZ diameter in patients with DR versus normal healthy controls, as well as absence of normal orientation of the angle of the maximum FAZ diameter in DR patients due to the irregular configuration of the FAZ. Balaratnasingam et al. [40] recorded a significant correlation between enlargement of FAZ and poor visual prognosis in patients with DR. They also found that this positive correlation is modulated by patient's age, such that an increase in patient's age is associated with poorer vision. Table 1 lists the average areas of the FAZ in both normal and DR cases.

Table 1. Average areas of FAZ in both normal and DR cases.

Study	No. of Patients	Age	SCP-FAZ (Control) (mm ²)	SCP-FAZ (DR) (mm ²)	DCP-FAZ (Control) (mm ²)	DCP-FAZ (DR) (mm ²)
Takase et al. [34]	20	65.8 ± 8.7	0.25 ± 0.06	0.38 ± 0.11	0.38 ± 0.11	0.56 ± 0.12
Salz et al. [20]	11	55.7 ± 10	0.3 ± 0.11	0.49 ± 0.19		
Suzuki et al. [35]	13	66.5 ± 10.4	0.31 ± 0.09	0.36 ± 0.13	0.45 ± 0.17	0.71 ± 0.2
Dupas et al. [36]	22	30 ± 6	0.20 ± 0.07	0.3 ± 0.11		

FAZ Morphology

Large individual variations can be detected by the evaluation of the FAZ area in both healthy [41,42] and diabetic [43] eyes. Using OCTA, FAZ morphological parameters (a metric called acirculatory index and axis ratio) were evaluated by Krawitz et al. [44] in patients with diabetes versus healthy controls. In OCTA, acircularity index (irregularity of FAZ) and axis ratio (the ratio of the maximum and minimum axes of a best-fit ellipse fitted to the FAZ) were found helpful in distinguishing between control subjects and diabetic subjects with no DR, NPDR, and proliferative diabetic retinopathy (PDR). Higher axis ratio and acircularity index are considered statistical significant indicators of retinopathy advanced stage. A strong negative correlation was found between FAZ acircularity index and BCVA. The change in the FAZ acircularity index in DR patients is probably because of the capillary dropout.

While quantification of FAZ area and shape has become increasingly common in the literature when characterizing sequelae of various retinal vascular diseases, there is another school of thought on the matter that calls into question the value of these metrics. One source of concern is that FAZ areas vary within the normal population. The value of various metrics to gauge the shape of the FAZ has also been called into question, as the clinical utility of varying distortions of “normal” shape have unclear clinical implications at the moment.

Vessel Density at the Macula

While macular vessel density is decreased in diabetics [45], there are conflicting data as to whether it is more reduced in the SCP than the DCP, vice versa or to approximately the same extent [46]. OCTA studies revealed a reduction of macular VD in diabetic patients with DR with positive correlation to the severity of DR [45]. Figure 2 shows reduction of VD in both DCP and SCP in a diabetic patient compared to control.

Zahid et al. [47] showed significantly lower VD in subjects of diabetes with DR when compared to healthy control eyes in both SCP and DCP. Dupas et al. [36] found that VD was reduced significantly in the SCP and DCP in diabetic subjects with DR with normal VA in comparison with healthy controls. This reduction is even more in patients of diabetes with DR and decreased VA (without macular edema). They concluded that the reduction in vessel density in patients with diabetes with DR is positively correlated with decreased

VA. Shen et al. [48] reported a significant reduction in the density of the vessels in the SCP in patients with diabetes with early DR when compared to healthy controls. However, no significant difference was found in retinal thickness between diabetic subjects and healthy controls. They concluded that compromised microvascular circulation precedes retinal structural changes. Table 2 lists the average VD in both normal and DR cases.

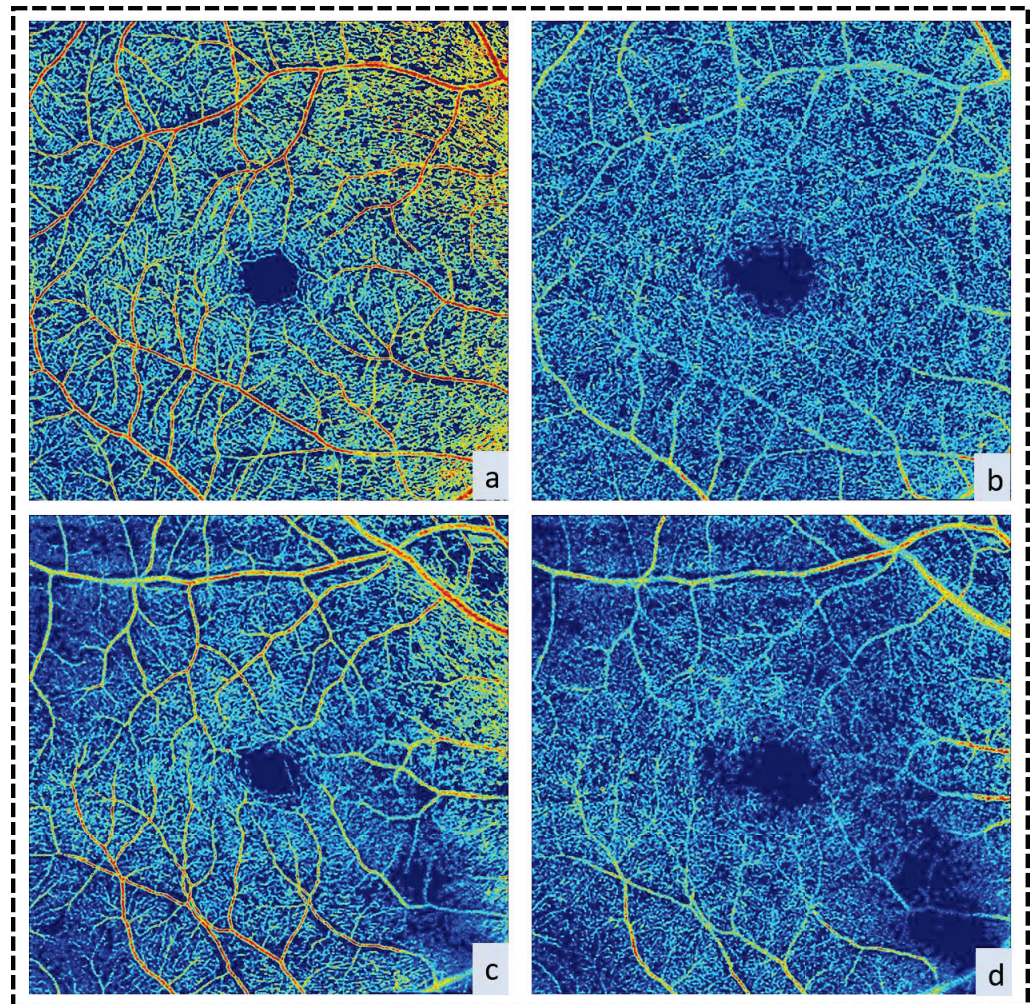


Figure 2. Vessels density. (a) SCP of normal control, (b) DCP of normal control, (c) SCP of the diabetic patient, and (d) DCP of a diabetic patient.

Table 2. The average VD in both normal and DR cases.

Study	No. of Patients	Age	SCP-VD (Control) (mm ²)	SCP-VD (DR) (mm ²)	DCP-VD (Control) (mm ²)	DCP-VD (DR) (mm ²)
Zahid et al. [47]	13	56.66 ± 12.65	55.6 ± 1.7	48.2 ± 4.6	60.6 ± 1.5	53.6 ± 3.2
Dupas et al. [36]	22	30 ± 6	49.1 ± 2.5	44.1 ± 2.5	50.6 ± 3.3	44.3 ± 3.2
Shen et al. [48]	49	56.4 ± 10.1	54.1 ± 2.1	47.82 ± 4.62		

Microaneurysms

Microaneurysms were identified on OCTA as a well-demarcated saccular or fusiform shapes of focally dilated capillaries in the SCP and DCP but mainly in the deep plexus [49]. Matsunaga et al. [50] compared the detection of microaneurysms in diabetic retinopathy using FA and OCTA. They found that only 23% of microaneurysms detected on FA were identified on OCTA. They also found variation in both shape and size of microaneurysms

detected by the two techniques. Microaneurysms appeared on FA as uniform round dots, while they appeared on OCTA smaller in size with multiple different shapes such as fusiform, solid round or round with dark centers.

Couturier et al. [12] compared the detection of microaneurysm in diabetic retinopathy using FA and OCTA. They found that 62% of microaneurysms detected on FA were identified on OCTA. They found that the number of microaneurysms detected per eye was 11.7 ± 7.1 on FA versus to 7.3 ± 3.9 on OCTA. Moreover, microaneurysms detected by OCTA were mainly in the DCP (4.4 ± 2.1 per eye) versus (2.9 ± 2.3 per eye) in the SCP.

Salz et al. [19] also compared the detection of microaneurysm in diabetic retinopathy using FA and OCTA. They found that 75% of microaneurysms detected with FA were identified on OCTA. They found that the number of microaneurysms detected per eye was 10.0 ± 6.9 on FA versus to 6.4 ± 4.0 on OCTA. Another study by Miwa et al. [51] found that OCTA can detect only $41.0 \pm 16.1\%$ of microaneurysms seen on FA images in eyes with DR. The detection of microaneurysm in OCTA and FA has some difference that may be explained by the nature of microaneurysms themselves, as some of them are not completely patent so red blood cells (detected by OCTA) may not pass into the microaneurysm but the smaller fluorescein molecules (detected by FA) still can pass into the microaneurysm [50]. It may also be explained by the fact that blood flow within some microaneurysm was too slow (less than 0.3 mm per second) to be detected by OCTA [12]. A third explanation is that some of the hyperfluorescent dots seen on FA (supposed to be microaneurysms) are actually curved or coiled capillaries as seen on OCTA [51]. This is a notable weakness of OCTA relative to traditional FA.

Cotton-Wool Spots

Cotton-wool spots detected as swelling of the nerve fiber layer on OCT have been shown to have impaired capillary perfusion on OCTA [50].

Intraretinal Microaneurysmal Abnormalities (IRMA)

OCTA shows IRMA as a group of looping vessels adjacent to areas of impaired capillary perfusion with their caliber greater than of surrounding capillaries [50].

Preretinal Neovascularization

PDR could be characterized by the preretinal neovascularization (neo-vascularization of the disc (NVD)) or neovascularization of the retina elsewhere (NVE)), which are abnormal, pathological vessels that protrude through the internal limiting membrane into the vitreous cavity caused by up-regulation of vascular endothelial growth factor (VEGF) and other angiogenic factors [52]. OCTA showed NVD as a group of disorganized vessels protruding from the disc into the vitreous [50]. Akiyama et al. [53] found that NVD arises from outside the physiological cupping into the vitreous cavity on OCTA. De Carlo et al. [54] found that preretinal neovascularization appears on OCTA as a fan of vessels extending into the vitreous bordering or overlying areas of retinal capillary dropout. The presence of NVD on OCTA is an indication for initiating treatment with anti-VEGF and/or panretinal photocoagulation. Multiple areas of NVE would also qualify as indications, although small areas of NVE that remain stable can often be safely observed.

Diabetic Macular Edema (DME)

Diabetic macular edema (DME) pathogenesis is linked to the blood barrier breakdown in retina with fluid leakage from microaneurysms. In diabetic eyes, VEGF is believed to be a main cause of hyperpermeability of retinal vasculature. Hence, anti-VEGF agents are usually considered the main and effective therapy for DME, which improves macular edema and visual prognosis in subjects with DME [55]. An OCTA study conducted by Haritoglou et al. [56] has found out that the high rate of the formation of macular microaneurysm (Mas) in diabetic patients is a predictor of the development of significant macular edema. Another OCTA study conducted by Hasegawa et al. [57] to analyze the relationship

between DME and microaneurysms distribution in different retinal layers concluded that there is a correlation between microaneurysms existing in the DCP and DME pathogenesis.

Mane et al. [58] studied the relation between the retinal capillary dropout areas in DME and the location of cystoid spaces. The authors found out that cystoid spaces theco-localized with areas of the capillary dropout, particularly in the DCP. There is no reperfusion that occurs after the DME resolution. OCTA has limitations in imaging of DME due to its inability to detect leakage. Hence, it cannot differentiate leaking from non-leaking microaneurysms. Another limitation is that there are defects of OCTA segmentation in the edematous macula. Decisions regarding treatment for DME are still primarily based on the presence of central cystoid spaces on structural OCT in combination with decreased visual acuity. OCTA does not typically play a role in this setting. However, severe capillary dropout in the macula that persists even with resolution of DME is something the treating clinician should consider. Macular ischemia can limit vision, and patients with center-involving DME whose vision fails to improve with resolution of edema often have significant macular ischemia that has damaged photoreceptors and reduced visual potential. In these cases, the clinician may consider withholding further treatment due to its futility. A further discussion of capillary dropout in the macula and abnormalities of the foveal avascular zone follows below.

2.1.2. Detection of Progression of DR FAZ Area

OCTA studies prove progressive enlargement of FAZ in a positive correlation with the severity of DR. Salz et al. [20] reported a positive correlation between enlargement of FAZ and increasing severity of DR. They reported that FAZ area was $0.30 \pm 0.11 \text{ mm}^2$ in normal healthy controls, then enlarged to $0.41 \pm 0.19 \text{ mm}^2$ in patients of diabetes without DR, then enlarged to $0.49 \pm 0.19 \text{ mm}^2$ in patients of diabetes with nonproliferative diabetic retinopathy (NPDR) and then enlarged to $0.76 \pm 0.16 \text{ mm}^2$ in diabetic patients with PDR. This conforms with the findings of Bhanushali et al. [59], who found out that FAZ area was $0.38 \pm 0.01 \text{ mm}^2$ in normal healthy controls, then enlarged to $0.45 \pm 0.03 \text{ mm}^2$ in diabetic patients with mild NPDR, then enlarged to $0.46 \pm 0.01 \text{ mm}^2$ in diabetic patients with moderate NPDR, then enlarged to $0.46 \pm 0.02 \text{ mm}^2$ in diabetic patients with severe NPDR and then enlarged to $0.47 \pm 0.02 \text{ mm}^2$ in diabetic patients with PDR.

Vessel Density at the Macula

OCTA studies prove a progressive reduction of VD in both DCP and SCP with increasing severity of DR. Bhanushali et al. [59] found reduction of VD in SCP from $49.7 \pm 0.55 \text{ mm}^2$ in normal healthy controls to $40.1 \pm 0.58 \text{ mm}^2$ in diabetic patients with mild NPDR, then reduced to $39.2 \pm 1.21 \text{ mm}^2$ in diabetic patients with moderate NPDR, then reduced to $38.5 \pm 0.76 \text{ mm}^2$ in diabetic patients with severe NPDR and then reduced to $38.9 \pm 1.38 \text{ mm}^2$ in diabetic patients with PDR. They also reported a reduction of VD in DCP from $53.1 \pm 0.73 \text{ mm}^2$ in normal healthy controls to $40.2 \pm 0.53 \text{ mm}^2$ in diabetic patients with mild NPDR, then reduced to $39.7 \pm 1.57 \text{ mm}^2$ in diabetic patients with moderate NPDR, then reduced to $39.4 \pm 0.68 \text{ mm}^2$ in diabetic patients with severe NPDR and then reduced to $39.2 \pm 0.94 \text{ mm}^2$ in diabetic patients with PDR.

Kim et al. [60] found that vessel density is reduced progressively in both DCP and SCP with severity increase of DR. They reported that the density of vessels in SCP was $0.42 \pm 0.01 \text{ mm}^2$ in normal healthy controls then reduced to $0.38 \pm 0.03 \text{ mm}^2$ in diabetic patients with mild NPDR, then reduced to $0.34 \pm 0.05 \text{ mm}^2$ in diabetic patients with severe NPDR and then reduced to $0.33 \pm 0.04 \text{ mm}^2$ in diabetic patients with PDR. They also found that vessel density in DCP was $0.43 \pm 0.01 \text{ mm}^2$ in normal healthy controls, then reduced to $0.42 \pm 0.01 \text{ mm}^2$ in diabetic patients with mild NPDR, then reduced to $0.40 \pm 0.05 \text{ mm}^2$ in diabetic patients with severe NPDR and then reduced to $0.39 \pm 0.03 \text{ mm}^2$ in diabetic patients with PDR. Figure 3 shows a progressive reduction of vessel density with the advancement of the stage of DR.

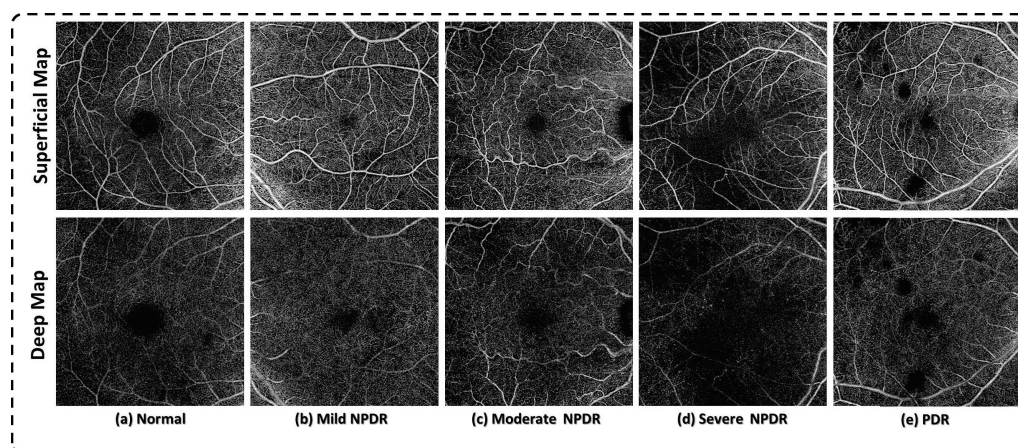


Figure 3. DR progression. A progressive reduction of vessel density with the advancement of the stage of DR.

2.1.3. Early Detection of DR

Microvascular damage occurs prior to the observation of retinopathy in clinical examination or fundus photography [61]. The initial diagnosis of NPDR usually detects DR at a relatively advanced stage of microscopic vascular changes, which were not clinically or angiographically detectable as proven by histological studies of cadaver eyes in humans [62].

The early detection of DR is effective in avoiding severe loss of vision in diabetic patients [63]. Early microvascular changes in diabetic retina in patients with no DR has been studied using OCTA. OCTA, being a non-invasive imaging modality, may be considered a very helpful tool for clinical screening of eyes of patients of diabetes with DR [64].

FAZ Area

Several studies (de Carlo et al. [65], Takase et al. [34], Suzuki et al. [35], Dimitrova et al. [66], Vujosevic et al. [67]) have demonstrated enlargement of FAZ area in diabetic patients regardless of DR existence. De Carlo et al. [65] reported enlargement of FAZ in healthy controls compared to the eyes of diabetic patients without DR.

Takase et al. [34] revealed enlargement of FAZ in the SCP in healthy controls compared to the eyes of diabetic patients without DR and enlargement of FAZ in the DCP in healthy controls compared to the eyes of diabetic patients without DR.

Suzuki et al. [35] revealed enlargement of FAZ in the SCP in healthy controls compared to the eyes of patients of diabetes without DR and enlargement of FAZ in the DCP in healthy controls compared to the eyes of diabetic patients without DR.

Dimitrova et al. [66] revealed enlargement of FAZ in the SCP in healthy controls compared to the eyes of diabetic patients without DR. Vujosevic et al. [67] revealed enlargement of FAZ in the SCP in healthy controls compared to the eyes of patients of diabetes without DR and enlargement of FAZ in the DCP in healthy controls compared to the eyes of diabetic patients without DR. Other studies (Carnevali et al. [46], Simonett et al. [31], Scarinci et al. [68], Cao et al. [64]) reported no statistical significance of the difference in FAZ area in the SCP between diabetic subjects without DR and normal healthy controls. Table 3 lists the average areas of the FAZ in both normal and early DR cases.

Table 3. Average areas of FAZ in normal and early DR cases.

Study	No. of Patients	Age	SCP-FAZ (Control) (mm ²)	SCP-FAZ (DR) (mm ²)	DCP-FAZ (Control) (mm ²)	DCP-FAZ (DR) (mm ²)
de Carlo et al. [65]	39	60 ± 20.55	0.28 ± 0.13	0.34 ± 0.10		
Takase et al. [34]	24	62.9 ± 9.8	0.25 ± 0.06	0.37 ± 0.07	0.38 ± 0.11	0.54 ± 0.13
Salz et al. [20]	11	55.7 ± 10	0.3 ± 0.11	0.41 ± 0.19		
Suzuki et al. [35]	14	66.5 ± 10.4	0.31 ± 0.09	0.36 ± 0.13	0.45 ± 0.17	0.70 ± 0.2
Dimitrova et al. [66]	23	69 ± 9.01	0.31 ± 0.10	0.37 ± 0.11		
Vujosevic et al. [67]	60	57.4 ± 15.4	0.28 ± 0.13	0.35 ± 0.12	0.36 ± 0.14	0.49 ± 0.15

Vessel Density at the Macula

One of the early characteristics of microvascular alteration in the retina of patients of diabetes is a reduction of VD. This reduction may be due to the alteration of retinal neurovascular autoregulation, which regulates blood flow in response to metabolic demands [69].

Some studies (Carnevali et al. [46], Simonett et al. [31], Scarinci et al. [68]) reported a statistical significance of the reduction of VD in DCP but not in SCP in diabetic eyes without DR when compared to healthy control eyes. Several studies (Dimitrova et al. [66], Cao et al. [64], Zeng et al. [70]) found a statistically significant reduction of VD in both DCP and SCP in diabetic subjects without DR as compared to normal healthy subjects. Furthermore, they reported no significant correlation between average VD and duration of diabetes or HBA1c level.

Rosen et al. [71] found that perfused capillary density (PCD) is elevated in diabetic subjects with no DR as compared to healthy subjects, and they suggested that PCD can be used as a preclinical biomarker of diabetic microvascular disease. The different findings between these studies may be related to the specific segmentation method employed. Rosen et al. [71] selectively isolated capillaries from non-capillary blood vessels, and their results revealed increased perfused capillary density. They suggested that this was an autoregulatory response to increased metabolic demand. Other authors [31,46] have not done that, which may explain their results of decreased vessel density in DCP.

Chen et al. [72] investigated fractal dimensions using OCTA in type 2 diabetic patients without DR to characterize the macular microvascular network. They reported diminished fractal dimensions in DCP in diabetic patients without DR as compared to healthy controls. Table 4 lists the average VD in both normal and early DR cases.

Table 4. The average VD in both normal and early DR cases.

Study	No. of Patients	Age	SCP-VD (Control) (mm ²)	SCP-VD (DR) (mm ²)	DCP-VD (Control) (mm ²)	DCP-VD (DR) (mm ²)
Carnevali et al. [46]	25	22 ± 2				
Simonett et al. [31]	28	42.3 ± 8.6				
Scarinci et al. [68]	20	38.5 ± 12.4	51.5 ± 4.2	58.7 ± 3.6		
Dimitrova et al. [66]	29	69 ± 9.01	51.39 ± 13.05	44.35 ± 13.31	41.53 ± 14.08	31.03 ± 16.33
Cao et al. [64]	71	57.4 ± 13.5	55.72 ± 2.43	51.34 ± 4.09	62.10 ± 2.11	57.66 ± 5.73
Zeng et al. [70]	66	58.77 ± 12.3	50.42 ± 3.73	48.12 ± 4.01	52.71 ± 6.56	48.62 ± 6.39

2.2. Age-Related Macular Degeneration (AMD)

AMD is a primary cause of blindness of adults above 50 years old in developed countries [73]. Neovascular AMD represents nearly 10% of AMD cases [74]. The onset of neovascular AMD determines the progress of the development of AMD from intermediate non-exudative to late exudative. Neovascular AMD refers to the abnormal growth of new vessels either underneath the RPE (neovascularization type 1), between the retina and the

RPE (neovascularization type 2), or starting within the retina (neovascularization type 3). Types 1 and 2 neovascularization are known as choroidal neovascularization (CNV) as they are derived from the choroidal circulation [75]. However, type 3 neovascularization refers to the retinal angiomatous proliferation as it arises initially from retinal circulation [76]. CNV onset in AMD was determined by macular exudation onset, which is recognized by either the leakage during FA [77], the existence of macular fluid in OCT [78], or the existence of vascular flow abnormal pattern in OCTA [79]. The most popular category of exudative AMD is type 1 CNV [76].

OCTA is also used in imaging the neovascular membrane inside the macula non-invasively. Even if there is no exudation, in OCTA, CNV type 1 is shown as vessels network located between the Bruch's membrane and the retinal pigment epithelium (RPE) [80], whereas CNV type 2 is visualized as vessels network in the normally avascular outer retina [81]. Furthermore, type 3 neovascularization is visualized as a discrete high flow linear structure that extends from middle layers in the retina into the deep retina and occasionally also past the RPE [82]. In Figure 4, an OCTA of an AMD patient showing abnormal vessels in the choriocapillaris layer and the choroid is shown.

The sign of activity of CNV on FA is the leakage existence. OCTA is unable to evaluate the existence of leakage or exudation, but it can potentially differentiate active from inactive CNV by changes in the pattern of the vasculature. Active CNV appears on OCTA as a branching and well-defined anastomosing tangle of vessels surrounded by dark halo corresponding to blood, exudation or sub-retinal fibrosis. Inactive CNV appears on OCTA as large mature vessels without anastomosis [83]. These distinctions are still not entirely clear cut, and further study is ongoing.

OCTA is considered to be better than FA in identifying neovascular membranes due to the absence of vascular obscuration by leakage from new vessels, which is typically seen on FA [84]. OCTA could detect CNV type 1 in 67–100% of cases in comparison with FA [85]. SS-OCTA (wavelength 1050 nm) is better than SD-OCTA (wavelength 840 nm) in visualization of CNV because of the better penetration of the former into the choroid [86]. Cases of dense subretinal hemorrhage secondary to CNV present a distinct challenge for OCTA, as well as often FA. These hemorrhages block penetration of light, and thus the underlying neovascular membranes and choriocapillaris cannot be imaged in these circumstances.

Type 1 CNV appears on the en-face OCTA as a well-defined entanglement of blood vessels while it appears on cross-sectional OCTA as intrinsic flow in sub-RPE space [87], while type 2 CNV appears on cross-sectional OCTA as hyper-reflective material with the intrinsic flow in the sub-retinal space with thicker main vessel branch that is connected to the choroid. The neovascular membrane is surrounded by a dark halo corresponding to blood, exudation or sub-retinal fibrosis [88]. Mixed CNV type 1 and type 2 lesions appear on cross-sectional OCTA as abnormal intrinsic flow above and below the RPE. Mixed CNV type 1 and type 2 lesions can be visualized on en-face OCTA by varying the segmentation depth, so the component of each type can be visualized on different slabs [89]. Type 3 neovascularization appears on the en-face OCTA as a tangle of blood vessels originating from the DCP in the outer retinal slab while, it appears on the cross-sectional OCTA as a hyper-reflective vascular structure with intrinsic flow extending from the outer retina slab into the inner retina slab [88].

Farecki et al. [90] differentiated types of CNV using OCTA. Authors found that CNV type 1 appears larger and less demarcated with predominant visibility on the choriocapillaris slab while CNV type 2 appears smaller and better demarcated with more visibility towards the outer retina slab. Quantifying the neovascular networks extent in CNV is very important for its well-known prognostic value [91]. The study conducted by Costanzo et al. [92] has held a comparison between the CNV type 1 size that is produced using OCTA and ICGA. Results showed that OCTA and ICGA are comparable, as they could provide information on CNV type 1 both quantitatively and qualitatively with good reproducibility and inter-user agreement. This conforms with the results of Amoroso et al. [93] and Lindner et al. [9].

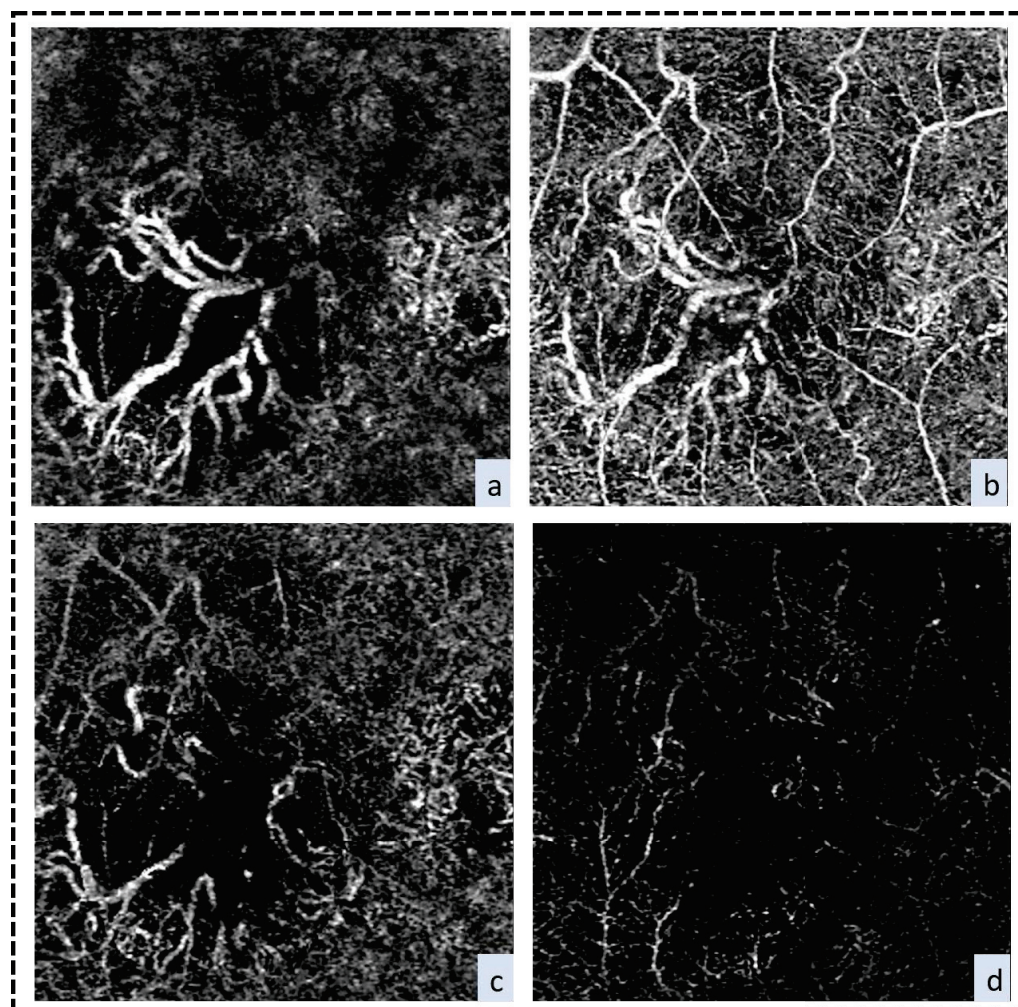


Figure 4. AMD. OCTA scan showing different plexuses for an AMD subject: (a) choroid layer, (b) whole retina, (c) Choriocapillaris layer, and (d) avascular layer.

A potential risk exists for CNV developing in eyes of individuals who have unilateral CNV. This risk varied from 6% to 42% in different studies (Palejwala et al. [79], Yanagi et al. [94], Roisman et al. [95], Amoroso et al. [93], Lindner et al. [7], De Oliveira Dias et al. [96] Treister et al. [97]). In these studies, authors explained the various factors that affect the subclinical CNV prevalence such as the duration and severity of AMD. The subclinical CNV in fellow eyes in the first year has its prevalence more than doubled as reported in the second-year follow-up [98].

Kuehlewein et al. [82] studied the response of CNV membranes to anti-VEGF using OCTA. They showed that after treatment, the size and the density of vessels of the neovascular membrane were significantly reduced. These results conform with the findings of Pilotto et al. [99], who revealed a reduction in the size of neovascular membrane 48 h after treatment. However, there was no change found in the main central trunk of feeder vessels. According to Bellou et al. [100], the main central trunk of feeder vessel might resist anti-VEGF therapy because of the protection provided by the pericytes overlying its endothelial cells, while the branching vascular network lacks the protective pericytes. However, they are more responsive to anti-VEGF therapy.

OCTA can directly and non-invasively visualize the neovascular membrane in the form of the thick central feeder vessel with vessels radiating from the lesion's center in all directions [86]. It can also monitor changes in this membrane, which precede the onset of exudation. It may be in the form of increase in flow in the feeder vessels or increase in the area of the neovascular membrane [7,101]. This can be very helpful in the management

of neovascular AMD, which is an indication for treatment with intravitreal anti-VEGF to suppress exudation. OCTA imaging can modify the current strategies (“treat and observe” or “treat and extend”) for neovascular AMD treatment [102].

Spaide [103] studied the appearance of the CNV vasculature, which is treated with injections of recurrent intravitreal anti-VEGF in eyes of 17 neovascular AMD subjects using OCTA. The finding stated that diameter of the vessel in the neovascular membrane remained larger than the normal vessels even after the treatment, which antagonizes the normalization hypothesis of blood vessels in the eyes that are treated using repeated intravitreal anti-VEGF.

The change in the size of the neovascular membrane in CNV patients in response to intravitreal anti-VEGF has been studied with OCTA. Cocas et al. [89] found a reduction of the size of the neovascular membrane over a follow up period of 4 weeks. Kuehlewein et al. [82] found no change of the size of the neovascular membrane over a 3-months follow up period. Xu et al. [104] found enlargement of the neovascular membrane in 80% of cases over a 12-month follow-up period, with doubling of the size of the membrane in 27% of patients. OCTA is particularly effective at detecting quiescent CNV or subclinical CNV. This is characterized by the presence of vessels with flow within drusenoid PEDs. In these cases, structural OCT will detect the drusenoid PEDs but no fluid or other OCT features suggestive of CNV. In the absence of exudation and clinical decreases in vision, these cases can be safely observed, but closer monitoring of these patients is indicated. These vessels could begin to exude fluid at almost any time, and the typical 6 month follow up schedule that is typical of dry AMD patients would not be appropriate in these cases. In patients with exudative AMD with active exudation, management decisions are primarily still based on structural OCT findings. CNV-complicating chorioretinal inflammatory lesions and central serous chorioretinopathy forms another set of conditions that is somewhat beyond the scope of this survey. OCTA is an excellent imaging modality in these cases, perhaps even the best, as it can distinguish between inflammatory lesions with and without vessels and identify CNV in areas of CSR pathology, when other imaging modalities are often unhelpful because these lesions cause leakage and OCTA abnormalities with or without CNV.

2.3. Retinal Vein Occlusion

Retinal vein occlusion (RVO) is ranked the second most common vascular disorder in retina after DR with significant visual impairment. Hypertension, open-angle glaucoma, smoking, thrombophilic disorders and diabetes are among the basic risk factors of RVO [105]. Macular ischemia or macular edema is the leading cause of central vision loss [106] in addition to its neovascular complications, including neovascular glaucoma and vitreous hemorrhage [107]. Figure 5 presents the capillary non-perfusion in DCP and SCP of RVO patient.

Almost all clinical and fluorescein angiographic findings that characterize retinal vein occlusions and its later sequelae are demonstrated by OCTA. The principal characteristics include collateral vessels formation, FAZ enlargement, decrease in capillary perfusion and venous dilation [108,109]. OCTA is actually superior in detecting irregularities of the FAZ and changes in DCP [110]. FA’s one advantage is that it shows physiologic leakage and has a wider field of view of the peripheral retina [1,111]. In general, visual acuity in BRVO correlates with macular edema, and vision improves as edema is reduced [112,113]. Reduction of ME alone, however, is not sufficient to produce good vision. The recovery of VA may be limited after ME resolution because of foveal photoreceptor damage secondary to macular ischemia, as concluded by OCT research [113,114]. Microvascular abnormalities, such as FAZ enlargement, microaneurysms, and capillary telangiectasia, in patients with RVO are seen more so in the DCP than in SCP [115–118]. The vessels’ architectural organization in the two plexuses could explain these findings. Transverse venules connect the SCP large venules directly to the DCP. The DCP in turn drains into the large superficial veins. Hence, in RVO patients, the intravascular pressure increase in large veins results in

hydrostatic pressure elevation with retinal perfusion reduction in DCP. A direct connection exists between the SCP and arterioles with high perfusion pressure and oxygenation in the retina. This probably helps to protect against the ischemic insult incurred by increased venous pressure in RVO [119].

Many studies (Wang et al. [120], Suzuki et al. [121], Kimura et al. [122], Cardoso et al. [123]) compared microvascular changes in the eye affected with RVO versus the fellow unaffected eye versus controls. They found reduction of the density of vessels in the DCP and SCP, reduction of choriocapillaris density, thickened subfoveal choroidal thickness, increased central macular thickness, and enlargement of the FAZ in eyes affected with RVO versus fellow unaffected eyes. They also found a reduction of the density of vessels in the DCP and SCP in the fellow unaffected eyes versus healthy controls.

OCTA images of RVO eyes have been analyzed by Spaide et al. [124], who concluded that the formation of cystoid spaces occurs at areas of disturbed vascular flow in the SCP. However, these cystoid spaces are absent or only present in areas of severely disturbed vascular flow in the DCP. No observed alterations in the pattern of the DCP or SCP occurred after resolution of cystoid spaces with treatment. Coscas et al. [117] concluded that in the SCP, cystoid spaces are more common in eyes with central retinal vein occlusion (CRVO), whereas in the DCP, they are more common in eyes with BRVO.

Several groups (Salles et al. [125], Balaratnasingam et al. [40], Samara et al. [126]) have reported enlargement of FAZ in eyes with CRVO. Salles et al. [125] reported enlargement of the mean FAZ area in the SCP from 0.25 in controls to 0.76 in patients with CRVO and enlargement of the mean FAZ area in the DCP from 0.49 in healthy controls to 1.12 in patients with CRVO. Samara et al. [126] reported enlargement of the mean FAZ area in the SCP from 0.28 in the fellow eye to 0.31 in the BRVO eye and enlargement of the mean FAZ area in the DCP from 0.41 in the fellow eye to 0.51 in the eye affected with BRVO.

Clinical studies (Salles et al. [125], Balaratnasingam et al. [40], Samara et al. [126], Wakabayashi et al. [115]) reported that the enlargement of FAZ is significantly correlated with poor visual prognosis in RVO patients. Balaratnasingam et al. [40] reported that this negative correlation is modulated by patient age such that an increase in patient age correlates with poorer vision. Salles et al. [125] reported that poor visual prognosis is directly proportional to the size of FAZ in the SCP but not in the DCP.

Several clinical studies (Winegarner et al. [127], Wakabayashi et al. [115], Ghashut et al. [128]) have studied the relationship between retinal perfusion and visual prognosis in eyes with RVO after ME resolution using anti-VEGF therapy. They reported a significant positive correlation between pre-treatment retinal perfusion and visual acuity at last follow up. Thus, OCTA is able to provide visual prognostic information for patients with RVO.

Using OCTA, Shiihara et al. [129] studied the relationship between morphological parameters (axial ratio and acircularity index) of the FAZ and BCVA in eyes with BRVO. Results demonstrated that acircularity index is not significantly correlated to BCVA in RVO. However, axial ratio (also called axis ratio) is significantly correlated to BCVA. Their finding suggests that the FAZ's morphological characteristics are more valuable visual prognostic indicators than the FAZ size alone in RVO eyes.

Collateral vessels in the retina tend to arise after BRVO more frequently than they happen after CRVO. Collaterals are enlarged, existing capillaries that bypass venous obstruction that is driven by hemodynamic and hydrostatic forces. Usually, these vessels develop within weeks of RVO [130]. Collateral vessels course through DCP but not in the SCP, which supports the serial arrangement of the DCP and SCP, with venous drainage predominantly coursing through the DCP [131]. Freund et al. [132] used OCTA to study the location of the collateral vessels that are associated with BRVO. They are curvilinear, dilated channels that connect veins across the horizontal raphe or veins on opposite sides of an occluded venous segment inside the same hemisphere of the retina. This conforms with the findings of Arrigo et al. [133] that the collateral vessels are located in the DCP, representing retinochoroidal anastomosis starting from the superficial retinal capillaries and reaching the choriocapillaris and choroidal vessels to bypass the site of occlusion.

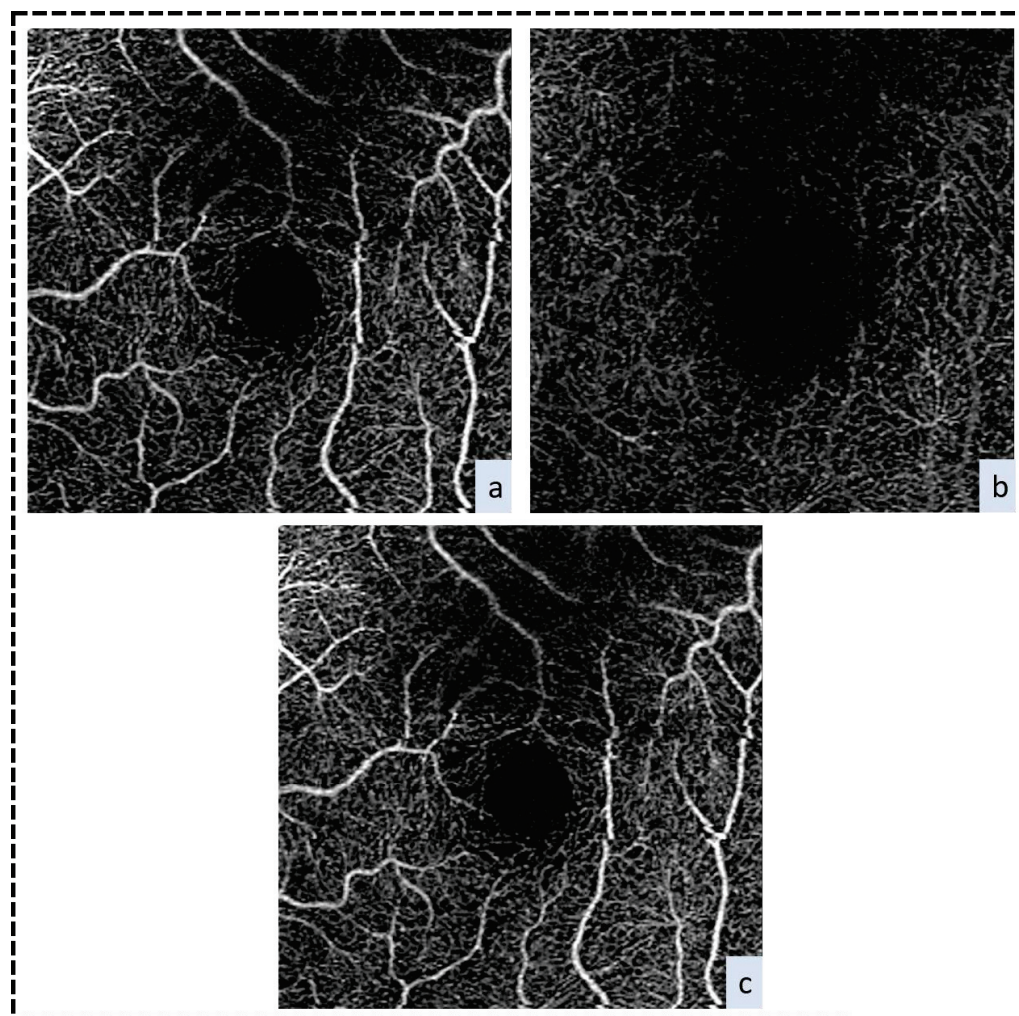


Figure 5. RVO. OCTA scan showing various plexuses for RVO subject: (a) superficial plexus, (b) deep plexus, (c) whole retina.

With BRVO eyes, Suzuki et al. [134] used OCTA to analyze collateral vessels and how they are associated with visual outcomes and ME. They found that collaterals were observed more frequently in eyes with major BRVO or ischemic BRVOS. Furthermore, one-third of the collaterals were found to leak fluid, and MAs were found inside all leaky collaterals. In eyes with collaterals, ME resolves quicker than in eyes that do not have collaterals; however, no significant difference was found. While average baseline central retinal thickness (CRT) is significantly higher in eyes with collaterals, the presence of collateral vessels appears to have no effect on visual outcomes. One of the major complications of ischemic RVO is neovascularization of the retina, which takes the form of neovascularization of the disc (NVD) or neovascularization elsewhere (NVE). Retinal ischemia can even drive the formation of NV in the anterior segment of the eye, causing neovascular glaucoma (NVG), a particularly aggressive form of glaucoma [135]. NV is highly abnormal, and these vessels can bleed spontaneously, causing vitreous hemorrhage and sudden vision loss, or they can scar, causing tractional retinal detachment. An OCTA study by Sogawa et al. [21] has analyzed NVE growth in an eye with hemi-CRVO. They found that OCTA can clearly visualize NVE growth and its detailed microvasculature. Identifying NV on OCTA is an indication for initiating or continuing anti-VEGF treatment or beginning panretinal photocoagulation. Development of collateral vessels is not an indication for anti-VEGF treatment.

Many of the manifestations of RVO have been attributed to increased levels of intraocular vascular endothelial growth factor (VEGF) [135]. VEGF drives both angiogenesis,

resulting in NV formation, and incompetence of normal capillaries, causing macular edema. Intravitreal anti-VEGF agents have become the mainstay of ME treatment, but this edema usually recurs at the same location of cystoid spaces after reduction of intraocular level of these agents [136]. Clinical studies (Spaide et al. [136], Falavarjani et al. [137], Winegarner et al. [138]) have reported no significant improvement in retinal perfusion or FAZ area in eyes with RVO after treatment with intravitreal anti-VEGF therapy and resolution of ME.

2.4. Retinal Artery Occlusion (RAO)

During the RAO acute phase, the capillary flow collapse results in intracellular edema, axoplasmic stasis, and retinal inner layers ischemic necrosis [6]. Usually, edema resolution is accompanied by the recanalization and reperfusion of the the obstructed retinal artery over the course of several weeks, but the infarction of the inner retina results in profound vision loss. Ultimately, the retina is left atrophic and with persistent vessel narrowing [29].

The retinal arterioles, which are arranged in two layers that are morphologically distinct, have a vital role in autoregulating blood flow in the retina. The superficial retinal capillary plexus exists at the nerve fiber layer close to the disk (radial parapapillary capillaries); however, it is present predominantly inside the ganglion cell layer in the central macular region. The DCP consists of intermediate and deep plexuses existing at inner and outer planes of the inner nuclear layer, respectively. Perpendicularly oriented vessels connect these capillary layers, which could be affected disproportionately by the ischemic vascular disease. Capillary plexus ischemia in RAO might occur in one or more inner layers of the retina resulting in ischemic edema, axoplasmic stasis and even death of the cells in the nonperfused region. These vascular layers could be affected differently by the severity of intracellular edema (there is capillary leakage or edema on OCT in RAOs), and the depth and area of capillary nonperfusion of the retina. In addition, the visual prognosis could be affected by the breadth of retinal capillary ischemia [139].

Branch retinal artery occlusion (BRAO) usually develops during the sixth or seventh decade of life as unilateral, painless vision loss in the visual field corresponding to the territory of the obstructed artery [140]. Montage OCTA is a technique that unites OCTA images of adjacent retinal regions to provide a wide field of view while preserving the microvascular details [6]. de Castro-Abeger used montage OCTA to evaluate a case with BRAO. Montage of OCTA comprise OCT angiograms segmented between Bruch's membrane and the inner limiting membrane (ILM). This uncovered severe decreased flow distal to the obstruction and a very distinct border of capillary non-perfusion. Capillary non-perfusion in the retina could be easily discerned in OCTA more than in FA due to the OCTA absence of choroidal flush [141].

Bonini Filho et al. [142] studied the retina's microvasculature in nonarteritic RAO eyes using OCTA and FA. They found that OCTA imaging observed a vascular perfusion decrease in deep and superficial retinal capillary plexus, which corresponded to the delayed perfusion areas in FA imaging. They also revealed that it is sensitive for the characterization of the extent of macular ischemia and for monitoring changes in the vascular flow within the course of the disease.

Cases with central retinal artery occlusion (CRAO) are at a higher risk of ocular neovascularization, so there is a recommendation for the retinal vasculature follow-up [143]. This is one of the important values of OCTA in follow up of cases with CRAO.

3. Optical Nerve Diseases

3.1. Glaucoma

Glaucoma is a main cause of irreversible blindness worldwide [144]. Glaucoma is a multifactorial optic neuropathy of unknown etiology [145]. Elevated intraocular pressure (IOP) is one of the risk factors for developing glaucoma, but it is not a sine qua non of the disease, as many patients diagnosed with glaucoma are found to have normal IOP levels at the time of diagnosis. One theory regarding the pathogenesis of glaucoma is that

it is vascular in origin [146]. Studying ocular microcirculation in glaucoma is challenging because of the difficulty in observing the microvasculature directly inside the retina's discrete layers and the optic nerve head (ONH) [147]. Fortunately, OCTA could potentially help in understanding the microvascular circulation role in the ONH and retina [6,148]. The OCTA is able to provide a 3-D visualization of the vasculature of the ONH from the disc surface to the lamina cribrosa, so it can be used as a diagnosis and evaluation of glaucoma or glaucoma suspects [149].

Yarmohammadi et al. [150] have presented a study to compare OCTA performance versus spectral-domain (SD)-OCT's in differentiating between glaucoma suspects, glaucoma patients, and healthy subjects. The results showed that both ONH density of vessels (OCTA) and the RNFL thickness (SD-OCT) have comparable diagnostic accuracy in differentiating between glaucomatous eyes and healthy eyes.

Evaluation of optic disc perfusion by OCTA allows calculation of the optic disc flow index, which has high sensitivity and specificity in diagnosing glaucomatous versus normal eyes. The value of the optic disc flow index has significant correlation to visual field changes but is not correlated to changes in the thickness of the retinal nerve fiber layer (RNFL). Additionally, values of the flow index can guide the decision to treat glaucoma suspects or ocular hypertensive patients [149].

OCTA studies found reduction of microvasculature at the optic disc (Jia et al. [149], Wang et al. [151], Yip et al. [152], Moghimi et al. [153]) in the peripapillary region (Liu et al. [148], Yip et al. [152], Yarmohammadi et al. [154], Mammo et al. [155], Akagi et al. [156], Suwan et al. [157], Scripsema et al. [158], Suh et al. [159]) and in the macula (Yip et al. [152], Moghimi et al. [153], Yarmohammadi et al. [160], Shoji et al. [161], Takusagawa et al. [162]) in glaucoma patients.

Jia et al. [149] used OCTA to assess optic disc perfusion in 35 subjects (11 glaucomatous, 24 controls). They found a reduction in optic disc flow index from 0.16 ± 0.01 in normal healthy controls to 0.12 ± 0.02 in glaucomatous patients. Moreover, this reduction in optic disc perfusion is correlated with visual field defect. This conforms with the findings of Wang et al. [151], who revealed a reduction in optic disc perfusion correlated with RNFL thickness, ganglion cell complex thickness, severity of glaucoma stage, and visual field mean deviation.

Yip et al. [152] noted a reduction of vessel density in the optic nerve head, peripapillary capillaries in 24 glaucomatous eyes versus 29 normal eyes using OCTA. They also found that the vessel density is reduced at the macular region at the SCP, DCP, outer retina, and choroid in glaucomatous patients versus controls. Moghimi et al. [153] found progressive reduction of macular VD and optic nerve head VD in 83 glaucoma patients using OCTA with a 2-year follow-up period. This progressive reduction of VD is correlated with thinning of the RNFL and VF loss.

Yarmohammadi et al. [154] studied the relation between density of vessels and visual field loss in glaucoma using OCTA. They revealed a positive correlation between reduction of peripapillary density of vessels and progression of visual field loss. However, there is no significant correlation between reduction of retinal nerve fiber thickness and visual field loss. They concluded that vascular-functional correlation is more important than structural-functional correlation. This is consistent with the results of Scripsema et al. [158], Yarmohammadi et al. [160], and Wang et al. [151]. Mammo et al. [155] investigated peripapillary VD in glaucoma patients using OCTA. They showed a reduction in peripapillary VD in areas corresponding to RNFL thinning on OCT scans and VF defect on Humphery perimetry. This vascular-functional correlation is explained by the fact that reduced vascular supply to retinal ganglion cells and their axons is the stage that precedes the death of ganglion supply. Therefore, OCTA detection of diminished vascular density is an early indicator of progression of the disease [163].

Akagi et al. [156] investigated peripapillary VD in 60 eyes with glaucoma and hemi-field VF defects using OCTA. A reduction was detected in the peripapillary VD that corresponds to the hemi-field VF defects in glaucomatous eyes that were either non-highly

myopic or highly myopic. Additionally, they found a reduction in the density of the optic disc vessel that corresponds to the hemi-field VF defects in non-highly myopic glaucomatous eyes, but not in highly myopic glaucomatous eyes.

Suh et al. [159] assessed peripapillary VD in 41 glaucomatous eyes with focal lamina cribrosa (LC) defect versus 41 glaucomatous eyes without LC defect. They revealed that reduction of peripapillary VD is greater in glaucomatous eyes with LC defect and that reduction of VD is most marked at the LC defect location.

Suwan et al. [157] compared peripapillary VD among 43 eyes with exfoliation glaucoma (XFG), 33 eyes with exfoliation syndrome (XFS), 31 eyes with primary open angle glaucoma (POAG), and 45 control healthy eyes. They found that peripapillary VD decreases from the controls to the XFS to the POAG to the XFG progressively.

Yarmohammadi et al. [160] investigated peripapillary VD and macular VD in 58 glaucomatous patients with hemi-field VF defect using OCTA. Authors found a reduction of VD in the affected hemi-retina when compared with the unaffected hemi-retina. In addition, the VD of the unaffected hemi-retina of glaucoma eyes is reduced when compared with VD of healthy control eyes.

Shoji et al. [161] used OCTA to study the average change rate in macular VD in glaucoma patients. They studied eyes of 100 cases (30 glaucoma-suspect, 32 glaucomatous, 38 healthy). The results showed that the average macular VD reduction rate was significantly faster in glaucomatous eyes ($-2 : 23\%/y$) than in glaucoma-suspect ($-0 : 87\%/y$) than in healthy eyes ($-0 : 29\%/y$).

A study conducted by Takusagawa et al. [162] used projection-resolved OCTA to study macular perfusion defects in 33 glaucoma patients. They found that the SCP is affected more than the DCP in glaucomatous eyes. This effect on the SCP in glaucoma is logical, as the SCP supplies the RNFL, part of the inner plexiform layer (IPL) and ganglion cell layer (GCL), the anatomic layers that the glaucoma affects the most. Rao et al. [164] investigated the diagnostic significance of the density of vessels in different regions in OCTA images. They found that peripapillary VD is more specific than optic nerve VD or macular VD in diagnosis of glaucoma.

Venugopal et al. [165] conducted an OCTA-based comparison between the intrasession repeatability of peripapillary and density of macular vessel measurements in 65 eyes (35 glaucomatous, 30 normal). For every eye, authors used three macular scans and three ONH scans. The results showed that most measurements have similar repeatability for eyes that are either glaucomatous or normal.

Rao et al. [166] studied choroidal microvascular dropout (CMvD) prevalence in OCTA of 73 POAG eyes (32 with disc hemorrhage (DH), 41 without DH). Results observed a dropout in the choroidal microvascular of 17 eyes with DH (53 : 1%) and 13 eyes without DH (31 : 7%).

Jung et al. [167] conducted a comparative study using 46 eyes with glaucoma and studied the localization of retinal nerve fiber layer defects in red-free fundus photographs and OCT en-face images. They found that the localized RNFL defects detected in OCT en-face structural images of the superficial retinal layer is highly topographically correlated with the detected defects in red-free photographs.

In summation, OCTA has provided numerous insights into the connection between the peripapillary vasculature and severity of glaucoma. This suggests possible pathophysiologic mechanisms for glaucoma, a still poorly understood disease, despite its being the most common optic neuropathy in the world. Despite these gains in knowledge, the clinical implications for management of glaucoma patients with these findings are as yet unclear, and visual field changes, pachymetry, RNFL thickness, cup-to-disc ratio, and intraocular pressure remain the key variables in clinical management.

3.2. Optic Neuropathy

Anterior Ischemic Optic Neuropathy (AION) is known as the acute, severe and painless loss of vision. This visual loss occurs because of ischemia that affects the ONH anterior

part, which the deep optic nerve plexus supplies [168]. According to different clinical features and histopathology, AION is partitioned into distinct arteritic (AAION) and non-arteritic (NAION) types [169]. NAION pathophysiology's most accepted theory is the ONH insufficiency of the small vessel circulatory [170]. There are major risk factors such as diabetes mellitus, hypertension, optic disc crowded structure and hypercholesterolemia [171].

Balducci et al. [172] presented an OCTA study to analyze AAION and NAAION features and compare it with ICGA and FA in 4 subjects. One AAION patient and four NAAION subjects participated in the study. Examination of the subjects was conducted during two weeks after disease presentation. They found that the ischemic area boundary could be identified by OCTA at the level of the ONH in the AAION patient and in two of four NAAION cases, which is confirmed by the boundary of optic disc filling defects in FA. Additionally, OCTA succeeded in the identification of the ischemic area boundary at the level of the ONH in the remaining two cases (NAAION), whereas FA failed in that due to generalized leakage that causes defect in optic disc filling. Several OCTA studies (Ling et al. [173], Song et al. [174]) revealed reduction of VD of the NAION eyes optic disc compared to healthy eyes. Mayes et al. [175] revealed impairment of flow in both retinal and choroidal peripapillary capillaries in OCTA of acute or chronic NAION eyes. This conforms with Augstburger et al. [176] and Sharma et al. [177] studies.

4. Limitations of OCTA

OCTA is relatively new and has some limitations that might affect its usage in clinical practice. We review in brief some of these limitations and potential advancement of OCTA manufacturers to address these limitations.

OCTA's field of view is much smaller than that of FA. However, this limitation has been solved in many commercial OCTA devices (wide field OCTA) by using multiple techniques such as image montaging [18,178,179], OCT-based microangiography [180], akinetic swept source [104] and extended field imaging technique [122,181], which enabled up to 12×12 mm scanning areas. Commercial OCTA devices often struggle to obtain high-quality images through small pupils or moderate media opacities through which FA and OCT are able to transit. Image artifacts are common in clinical practice. OCT angiography can also mask laser scars since they are "no flow" areas [182]. As mentioned above, OCTA does not show active leakage either.

In addition, OCTA is unable to detect blood flow below the minimum threshold. This leads it to miss microaneurysm if blood flow within is below that detected by OCTA [12]. Furthermore, OCTA can mask laser scars since they are eminent "no flow" areas [182].

A limitation of SD-OCTA is its inability to demonstrate choroidal diseases such as CNV, but this limitation is not present in SS-OCTA, which has longer wavelength with deeper penetration into the choroid.

On the other hand, different types of artifacts, such as segmentation, blinks, motions, and projection, may influence interpretation and measurements in OCTA images [183]. Segmentation artifacts occur in many situations, so there could be a need for manual manipulation of images in these situations to optimize the vascular details to ensure optimal OCTA interpretation [184]. Blink artifact appears as a black line because the OCT signal could not reach the retina or the software; accordingly, no movement was detected. Motion artifact appears as white lines, which represent signal decorrelation over the entire b-scan. These artifacts usually appear in areas where there is heavy subject movement when the patient moves or loses fixation. This motion artifact has been corrected in many OCTA devices by implication of the motion tracking system [185].

Projection artifact happens when the large retinal vessels of the superficial vessel complex cast shadow on the deep vessel complex of the retina, making identification of the latter difficult. Moreover, blood vessels in the inner retina give a false shadow of blood vessels in the outer retina, which is normally avascular. A projection-resolved algorithm solved this problem to some extent [162]. One of the limitations of OCTA in the assessment

of the optic nerve vasculature is that it detects overall disc flow measurements without differentiating retinal circulation from the posterior ciliary artery [186].

5. Conclusions

OCTA is a new imaging technique for diagnosing diseases in retina and optic nerves. OCTA has advantages over other angiographic imaging techniques, FA and ICG, of being non-invasive, rapid and reliable. OCTA also has the advantage of providing three-dimensional images, allowing visualization of retinal and choroidal vasculature in different layers. OCTA has some disadvantages such as the limited field of view (which has been partly solved in some commercially available devices), inability to identify leakage, inability to detect blood flow below a certain level, and variable image quality in a real-world, clinical setting.

OCTA is a helpful imaging modality for diagnosing and monitoring different retinal and choroidal diseases, including age-related macular degeneration, diabetic retinopathy, retinal vein occlusion, retinal artery occlusion, ischemic optic neuropathy, and glaucomatous optic neuropathy. Although the technology is still in its infancy, further improvements in imaging quality, reduction of artifacts, improved transmission through opaque media, and increased affordability will lead likely to more widespread adoption of the technology. This, in turn, should allow for more rigorous characterizations of these disorders and others.

Author Contributions: Conceptualization, F.T., H.M., M.G., H.S.S. and A.E.-B.; Project administration, A.E.-B.; Supervision, H.S.S. and A.E.-B.; Writing—original draft, F.T., H.K., H.M., A.M., A.S., M.G., M.T.A., H.S.S. and A.E.-B.; Writing—review and editing, F.T., H.K., H.M., A.M., A.S., M.G., M.T.A., H.S.S. and A.E.-B. All authors have read and agreed to the published version of the manuscript.

Funding: This work is supported, in part, by the Abu Dhabi Award for Research Excellence (AARE) 2019.

Acknowledgments: This work is supported, in part, by the Abu Dhabi Award for Research Excellence (AARE) 2019.

Conflicts of Interest: The authors declare no conflict of interest.

References

1. Savastano, M.C.; Lumbroso, B.; Rispoli, M. In vivo characterization of retinal vascularization morphology using optical coherence tomography angiography. *Retina* **2015**, *35*, 2196–2203. [[CrossRef](#)] [[PubMed](#)]
2. Hwang, T.S.; Jia, Y.; Gao, S.S.; Bailey, S.T.; Lauer, A.K.; Flaxel, C.J.; Wilson, D.J.; Huang, D. Optical coherence tomography angiography features of diabetic retinopathy. *Retina* **2015**, *35*, 2371. [[CrossRef](#)] [[PubMed](#)]
3. Mahmud, M.S.; Cadotte, D.W.; Vuong, B.; Sun, C.; Luk, T.W.; Mariampillai, A.; Yang, V.X. Review of speckle and phase variance optical coherence tomography to visualize microvascular networks. *J. Biomed. Opt.* **2013**, *18*, 050901. [[CrossRef](#)] [[PubMed](#)]
4. Wei, E.; Jia, Y.; Tan, O.; Potsaid, B.; Liu, J.J.; Choi, W.; Fujimoto, J.G.; Huang, D. Parafoveal retinal vascular response to pattern visual stimulation assessed with OCT angiography. *PLoS ONE* **2013**, *8*, e81343. [[CrossRef](#)]
5. Chen, C.L.; Wang, R.K. Optical coherence tomography based angiography. *Biomed. Opt. Express* **2017**, *8*, 1056–1082. [[CrossRef](#)]
6. Spaide, R.F.; Klancnik, J.M.; Cooney, M.J. Retinal vascular layers imaged by fluorescein angiography and optical coherence tomography angiography. *JAMA Ophthalmol.* **2015**, *133*, 45–50. [[CrossRef](#)] [[PubMed](#)]
7. Jia, Y.; Bailey, S.T.; Wilson, D.J.; Tan, O.; Klein, M.L.; Flaxel, C.J.; Potsaid, B.; Liu, J.J.; Lu, C.D.; Kraus, M.F. Quantitative optical coherence tomography angiography of choroidal neovascularization in age-related macular degeneration. *Ophthalmology* **2014**, *121*, 1435–1444. [[CrossRef](#)] [[PubMed](#)]
8. Jia, Y.; Bailey, S.T.; Hwang, T.S.; McClintic, S.M.; Gao, S.S.; Pennesi, M.E.; Flaxel, C.J.; Lauer, A.K.; Wilson, D.J.; Hornegger, J. Quantitative optical coherence tomography angiography of vascular abnormalities in the living human eye. *Proc. Natl. Acad. Sci. USA* **2015**, *112*, E2395–E2402. [[CrossRef](#)]
9. Lindner, M.; Fang, P.P.; Steinberg, J.S.; Domdei, N.; Pfau, M.; Krohne, T.U.; Schmitz-Valckenberg, S.; Holz, F.G.; Fleckenstein, M. OCT Angiography–Based Detection and Quantification of the Neovascular Network in Exudative AMD. *Investig. Ophthalmol. Vis. Sci.* **2016**, *57*, 6342–6348. [[CrossRef](#)]
10. Conrath, J.; Giorgi, R.; Raccach, D.; Ridings, B. Foveal avascular zone in diabetic retinopathy: Quantitative vs qualitative assessment. *Eye* **2005**, *19*, 322. [[CrossRef](#)]

11. Arend, O.; Wolf, S.; Harris, A.; Reim, M. The relationship of macular microcirculation to visual acuity in diabetic patients. *Arch. Ophthalmol.* **1995**, *113*, 610–614. [[CrossRef](#)] [[PubMed](#)]
12. Couturier, A.; Mané, V.; Bonnin, S.; Erginay, A.; Massin, P.; Gaudric, A.; Tadayoni, R. Capillary plexus anomalies in diabetic retinopathy on optical coherence tomography angiography. *Retina* **2015**, *35*, 2384–2391. [[CrossRef](#)] [[PubMed](#)]
13. Staurengi, G.; Bottoni, F.; Giani, A. Clinical applications of diagnostic indocyanine green angiography. In *Retina*; Elsevier: Amsterdam, The Netherlands, 2013; pp. 51–81.
14. Johnson, R.N.; Fu, A.D.; McDonald, H.R.; Jumper, J.M.; Ai, E.; Cunningham, E.T.; Lujan, B.J. Fluorescein angiography: Basic principles and interpretation. In *Retina*, 5th ed.; Elsevier Inc.: Amsterdam, The Netherlands, 2012.
15. Manivannan, A.; Kirkpatrick, J.; Sharp, P.; Forrester, J. Novel approach towards colour imaging using a scanning laser ophthalmoscope. *Br. J. Ophthalmol.* **1998**, *82*, 342–345. [[CrossRef](#)]
16. Zawadzki, R.J.; Jones, S.M.; Pilli, S.; Balderas-Mata, S.; Kim, D.Y.; Olivier, S.S.; Werner, J.S. Integrated adaptive optics optical coherence tomography and adaptive optics scanning laser ophthalmoscope system for simultaneous cellular resolution retinal imaging. *Biomed. Opt. Express* **2011**, *2*, 1674–1686. [[CrossRef](#)]
17. Witmer, M.T.; Parlitsis, G.; Patel, S.; Kiss, S. Comparison of ultra-widefield fluorescein angiography with the Heidelberg Spectralis® noncontact ultra-widefield module versus the Optos® Optomap®. *Clin. Ophthalmol.* **2013**, *7*, 389. [[CrossRef](#)]
18. De Carlo, T.E.; Romano, A.; Waheed, N.K.; Duker, J.S. A review of optical coherence tomography angiography (OCTA). *Int. J. Retin. Vitro.* **2015**, *1*, 5. [[CrossRef](#)]
19. Kadomoto, S.; Muraoka, Y.; Ooto, S.; Miwa, Y.; Iida, Y.; Suzuma, K.; Murakami, T.; Ghashut, R.; Tsujikawa, A.; Yoshimura, N. Evaluation of macular ischemia in eyes with branch retinal vein occlusion: An optical coherence tomography angiography study. *Retina* **2018**, *38*, 272–282. [[CrossRef](#)]
20. Salz, D.A.; Talisa, E.; Adhi, M.; Moulton, E.; Choi, W.; Baumal, C.R.; Witkin, A.J.; Duker, J.S.; Fujimoto, J.G.; Waheed, N.K. Select features of diabetic retinopathy on swept-source optical coherence tomographic angiography compared with fluorescein angiography and normal eyes. *JAMA Ophthalmol.* **2016**, *134*, 644–650. [[CrossRef](#)]
21. Sogawa, K.; Nagaoka, T.; Ishibazawa, A.; Takahashi, A.; Tani, T.; Yoshida, A. En-face optical coherence tomography angiography of neovascularization elsewhere in hemicentral retinal vein occlusion. *Int. Med Case Rep. J.* **2015**, *8*, 263. [[CrossRef](#)]
22. Ogurtsova, K.; da Rocha Fernandes, J.; Huang, Y.; Linnenkamp, U.; Guariguata, L.; Cho, N.; Cavan, D.; Shaw, J.; Makaroff, L. IDF Diabetes Atlas: Global estimates for the prevalence of diabetes for 2015 and 2040. *Diabetes Res. Clin. Pract.* **2017**, *128*, 40–50. [[CrossRef](#)]
23. Terry, T.; Raravikar, K.; Chokrungravanon, N.; Reaven, P.D. Does aggressive glycemic control benefit macrovascular and microvascular disease in type 2 diabetes?: Insights from ACCORD, ADVANCE, and VADT. *Curr. Cardiol. Rep.* **2012**, *14*, 79–88. [[CrossRef](#)]
24. Yau, J.W.; Rogers, S.L.; Kawasaki, R.; Lamoureux, E.L.; Kowalski, J.W.; Bek, T.; Chen, S.J.; Dekker, J.M.; Fletcher, A.; Grauslund, J. Global prevalence and major risk factors of diabetic retinopathy. *Diabetes Care* **2012**, *35*, 556–564. [[CrossRef](#)] [[PubMed](#)]
25. Zhang, K.; Ferreyra, H.A.; Grob, S.; Bedell, M.; Zhang, J.J. Diabetic retinopathy: Genetics and etiologic mechanisms. In *Retina*; Elsevier: Amsterdam, The Netherlands, 2013; pp. 925–939.
26. Cheung, C.Y.; Ikram, M.K.; Klein, R.; Wong, T.Y. The clinical implications of recent studies on the structure and function of the retinal microvasculature in diabetes. *Diabetologia* **2015**, *58*, 871–885. [[CrossRef](#)] [[PubMed](#)]
27. Durham, J.T.; Herman, I.M. Microvascular modifications in diabetic retinopathy. *Curr. Diabetes Rep.* **2011**, *11*, 253–264. [[CrossRef](#)]
28. Hwang, T.S.; Gao, S.S.; Liu, L.; Lauer, A.K.; Bailey, S.T.; Flaxel, C.J.; Wilson, D.J.; Huang, D.; Jia, Y. Automated quantification of capillary nonperfusion using optical coherence tomography angiography in diabetic retinopathy. *JAMA Ophthalmol.* **2016**, *134*, 367–373. [[CrossRef](#)]
29. Mendis, K.R.; Balaratnasingham, C.; Yu, P.; Barry, C.J.; McAllister, I.L.; Cringle, S.J.; Yu, D.Y.J.I. Correlation of histologic and clinical images to determine the diagnostic value of fluorescein angiography for studying retinal capillary detail. *Investig. Ophthalmol. Vis. Sci.* **2010**, *51*, 5864–5869. [[CrossRef](#)]
30. Schwartz, D.M.; Fingler, J.; Kim, D.Y.; Zawadzki, R.J.; Morse, L.S.; Park, S.S.; Fraser, S.E.; Werner, J.S. Phase-variance optical coherence tomography: A technique for noninvasive angiography. *Ophthalmology* **2014**, *121*, 180–187. [[CrossRef](#)]
31. Simonett, J.M.; Scarinci, F.; Picconi, F.; Giorno, P.; De Geronimo, D.; Di Renzo, A.; Varano, M.; Frontoni, S.; Parravano, M. Early microvascular retinal changes in optical coherence tomography angiography in patients with type 1 diabetes mellitus. *Acta Ophthalmol.* **2017**, *95*, e751–e755. [[CrossRef](#)]
32. Bandello, F.; Corbelli, E.; Carnevali, A.; Pierro, L.; Querques, G. Optical coherence tomography angiography of diabetic retinopathy. In *OCT Angiography in Retinal and Macular Diseases*; Karger Publishers: Berlin, Germany, 2016; Volume 56, pp. 107–112.
33. Kim, D.Y.; Fingler, J.; Zawadzki, R.J.; Park, S.S.; Morse, L.S.; Schwartz, D.M.; Fraser, S.E.; Werner, J.S. Noninvasive imaging of the foveal avascular zone with high-speed, phase-variance optical coherence tomography. *Investig. Ophthalmol. Vis. Sci.* **2012**, *53*, 85–92. [[CrossRef](#)]
34. Takase, N.; Nozaki, M.; Kato, A.; Ozeki, H.; Yoshida, M.; Ogura, Y. Enlargement of foveal avascular zone in diabetic eyes evaluated by en face optical coherence tomography angiography. *Retina* **2015**, *35*, 2377–2383. [[CrossRef](#)]
35. Suzuki, K.; Nozaki, M.; Takase, N.; Kato, A.; Morita, H.; Ozeki, H.; Yoshida, M.; Ogura, Y. Association of Foveal Avascular Zone Enlargement and Diabetic Retinopathy Progression Using Optical Coherence Tomography Angiography. *J. Vitro. Dis.* **2018**, *2*, 343–350. [[CrossRef](#)]

36. Dupas, B.; Minvielle, W.; Bonnin, S.; Couturier, A.; Erginay, A.; Massin, P.; Gaudric, A.; Tadayoni, R. Association between vessel density and visual acuity in patients with diabetic retinopathy and poorly controlled type 1 diabetes. *JAMA Ophthalmol.* **2018**, *136*, 721–728. [[CrossRef](#)] [[PubMed](#)]
37. Freiberg, F.J.; Pfau, M.; Wons, J.; Wirth, M.A.; Becker, M.D.; Michels, S. Optical coherence tomography angiography of the foveal avascular zone in diabetic retinopathy. *Graefe's Arch. Clin. Exp. Ophthalmol.* **2016**, *254*, 1051–1058. [[CrossRef](#)]
38. Eladawi, N.; Elmogy, M.; Khalifa, F.; Ghazal, M.; Ghazi, N.; Aboelfetouh, A.; Riad, A.; Sandhu, H.; Schaal, S.; El-Baz, A. Early diabetic retinopathy diagnosis based on local retinal blood vessels analysis in optical coherence tomography angiography (OCTA) images. *Med. Phys.* **2018**, *45*, 4582–4599. [[CrossRef](#)]
39. Sandhu, H.S.; Eladawi, N.; Elmogy, M.; Keynton, R.; Helmy, O.; Schaal, S.; El-Baz, A. Automated diabetic retinopathy detection using optical coherence tomography angiography: A pilot study. *Br. J. Ophthalmol.* **2018**, *102*, 1564–1569. [[CrossRef](#)]
40. Balaratnasingam, C.; Inoue, M.; Ahn, S.; McCann, J.; Dhrami-Gavazi, E.; Yannuzzi, L.A.; Freund, K.B. Visual acuity is correlated with the area of the foveal avascular zone in diabetic retinopathy and retinal vein occlusion. *Ophthalmology* **2016**, *123*, 2352–2367. [[CrossRef](#)]
41. Chui, T.Y.; VanNasdale, D.A.; Elsner, A.E.; Burns, S.A. The association between the foveal avascular zone and retinal thickness. *Investig. Ophthalmol. Vis. Sci.* **2014**, *55*, 6870–6877. [[CrossRef](#)]
42. Zheng, Y.; Gandhi, J.S.; Stangos, A.N.; Campa, C.; Broadbent, D.M.; Harding, S.P. Automated segmentation of foveal avascular zone in fundus fluorescein angiography. *Investig. Ophthalmol. Vis. Sci.* **2010**, *51*, 3653–3659. [[CrossRef](#)]
43. Hilmantel, G.; Applegate, R.A.; Stowers, S.; Bradley, A.; Lee, B. Entoptic foveal avascular zone measurement and diabetic retinopathy. *Optom. Vis. Sci. Off. Publ. Am. Acad. Optom.* **1999**, *76*, 826–831. [[CrossRef](#)]
44. Krawitz, B.D.; Mo, S.; Geyman, L.S.; Agemy, S.A.; Scripsema, N.K.; Garcia, P.M.; Chui, T.Y.; Rosen, R.B. Acircularity index and axis ratio of the foveal avascular zone in diabetic eyes and healthy controls measured by optical coherence tomography angiography. *Vis. Res.* **2017**, *139*, 177–186. [[CrossRef](#)]
45. Samara, W.A.; Shahlaee, A.; Adam, M.K.; Khan, M.A.; Chiang, A.; Maguire, J.I.; Hsu, J.; Ho, A.C. Quantification of diabetic macular ischemia using optical coherence tomography angiography and its relationship with visual acuity. *Ophthalmology* **2017**, *124*, 235–244. [[CrossRef](#)] [[PubMed](#)]
46. Carnevali, A.; Sacconi, R.; Corbelli, E.; Tomasso, L.; Querques, L.; Zerbini, G.; Scordia, V.; Bandello, F.; Querques, G. Optical coherence tomography angiography analysis of retinal vascular plexuses and choriocapillaris in patients with type 1 diabetes without diabetic retinopathy. *Acta Diabetologica* **2017**, *54*, 695–702. [[CrossRef](#)] [[PubMed](#)]
47. Zahid, S.; Dolz-Marco, R.; Freund, K.B.; Balaratnasingam, C.; Dansingani, K.; Gilani, F.; Mehta, N.; Young, E.; Klifto, M.R.; Chae, B. Fractal dimensional analysis of optical coherence tomography angiography in eyes with diabetic retinopathy. *Investig. Ophthalmol. Vis. Sci.* **2016**, *57*, 4940–4947. [[CrossRef](#)] [[PubMed](#)]
48. Shen, C.; Yan, S.; Du, M.; Zhao, H.; Shao, L.; Hu, Y. Assessment of capillary dropout in the superficial retinal capillary plexus by optical coherence tomography angiography in the early stage of diabetic retinopathy. *BMC Ophthalmol.* **2018**, *18*, 113. [[CrossRef](#)] [[PubMed](#)]
49. Ishibazawa, A.; Nagaoka, T.; Takahashi, A.; Omae, T.; Tani, T.; Sogawa, K.; Yokota, H.; Yoshida, A. Optical coherence tomography angiography in diabetic retinopathy: A prospective pilot study. *Am. J. Ophthalmol.* **2015**, *160*, 35–44.e1. [[CrossRef](#)] [[PubMed](#)]
50. Matsunaga, D.R.; Jack, J.Y.; De Koo, L.O.; Ameri, H.; Puliafito, C.A.; Kashani, A.H. Optical coherence tomography angiography of diabetic retinopathy in human subjects. *Ophthalmic Surg. Lasers Imaging Retin.* **2015**, *46*, 796–805. [[CrossRef](#)] [[PubMed](#)]
51. Miwa, Y.; Murakami, T.; Suzuma, K.; Uji, A.; Yoshitake, S.; Fujimoto, M.; Yoshitake, T.; Tamura, Y.; Yoshimura, N. Relationship between functional and structural changes in diabetic vessels in optical coherence tomography angiography. *Sci. Rep.* **2016**, *6*, 29064. [[CrossRef](#)] [[PubMed](#)]
52. Muqit, M.M.; Stanga, P.E. Fourier-domain optical coherence tomography evaluation of retinal and optic nerve head neovascularization in proliferative diabetic retinopathy. *Br. J. Ophthalmol.* **2014**, *98*, 65–72. [[CrossRef](#)] [[PubMed](#)]
53. Akiyama, H.; Li, D.; Shimoda, Y.; Matsumoto, H.; Kishi, S. Observation of neovascularization of the disc associated with proliferative diabetic retinopathy using OCT angiography. *Jpn. J. Ophthalmol.* **2018**, *62*, 286–291. [[CrossRef](#)] [[PubMed](#)]
54. De Carlo, T.E.; Bonini Filho, M.A.; Baumal, C.R.; Reichel, E.; Rogers, A.; Witkin, A.J.; Duker, J.S.; Waheed, N.K. Evaluation of pre-retinal neovascularization in proliferative diabetic retinopathy using optical coherence tomography angiography. *Ophthalmic Surg. Lasers Imaging Retin.* **2016**, *47*, 115–119. [[CrossRef](#)] [[PubMed](#)]
55. Nguyen, Q.D.; Brown, D.M.; Marcus, D.M.; Boyer, D.S.; Patel, S.; Feiner, L.; Gibson, A.; Sy, J.; Rundle, A.C.; Hopkins, J.J. Ranibizumab for diabetic macular edema: Results from 2 phase III randomized trials: RISE and RIDE. *Ophthalmology* **2012**, *119*, 789–801. [[CrossRef](#)]
56. Haritoglou, C.; Kernt, M.; Neubauer, A.; Gerss, J.; Oliveira, C.M.; Kampik, A.; Ulbig, M. Microaneurysm formation rate as a predictive marker for progression to clinically significant macular edema in nonproliferative diabetic retinopathy. *Retina* **2014**, *34*, 157–164. [[CrossRef](#)]
57. Hasegawa, N.; Nozaki, M.; Takase, N.; Yoshida, M.; Ogura, Y. New insights into microaneurysms in the deep capillary plexus detected by optical coherence tomography angiography in diabetic macular edema. *Investig. Ophthalmol. Vis. Sci.* **2016**, *57*, OCT348–OCT355. [[CrossRef](#)]

58. Mané, V.; Dupas, B.; Gaudric, A.; Bonnin, S.; Pedinielli, A.; Bousquet, E.; Erginay, A.; Tadayoni, R.; Couturier, A. Correlation between cystoid spaces in chronic diabetic macular edema and capillary nonperfusion detected by optical coherence tomography angiography. *Retina* **2016**, *36*, S102–S110. [[CrossRef](#)]
59. Bhanushali, D.; Anegondi, N.; Gadde, S.G.; Srinivasan, P.; Chidambara, L.; Yadav, N.K.; Roy, A.S. Linking retinal microvasculature features with severity of diabetic retinopathy using optical coherence tomography angiography. *Investig. Ophthalmol. Vis. Sci.* **2016**, *57*, OCT519–OCT525. [[CrossRef](#)]
60. Kim, A.Y.; Chu, Z.; Shahidzadeh, A.; Wang, R.K.; Puliafito, C.A.; Kashani, A.H. Quantifying microvascular density and morphology in diabetic retinopathy using spectral-domain optical coherence tomography angiography. *Investig. Ophthalmol. Vis. Sci.* **2016**, *57*, OCT362–OCT370. [[CrossRef](#)]
61. Barot, M.; Gokulgandhi, M.R.; Patel, S.; Mitra, A.K. Microvascular complications and diabetic retinopathy: Recent advances and future implications. *Future Med. Chem.* **2013**, *5*, 301–314. [[CrossRef](#)]
62. Stitt, A.W.; Curtis, T.M.; Chen, M.; Medina, R.J.; McKay, G.J.; Jenkins, A.; Gardiner, T.A.; Lyons, T.J.; Hammes, H.P.; Simo, R. The progress in understanding and treatment of diabetic retinopathy. *Prog. Retin. Eye Res.* **2016**, *51*, 156–186. [[CrossRef](#)]
63. Kawasaki, R.; Akune, Y.; Hiratsuka, Y.; Fukuhara, S.; Yamada, M. Cost-utility analysis of screening for diabetic retinopathy in Japan: A probabilistic Markov modeling study. *Ophthalmic Epidemiol.* **2015**, *22*, 4–12. [[CrossRef](#)]
64. Cao, D.; Yang, D.; Huang, Z.; Zeng, Y.; Wang, J.; Hu, Y.; Zhang, L. Optical coherence tomography angiography discerns preclinical diabetic retinopathy in eyes of patients with type 2 diabetes without clinical diabetic retinopathy. *Acta Diabetol.* **2018**, *55*, 469–477. [[CrossRef](#)]
65. Talisa, E.; Chin, A.T.; Bonini Filho, M.A.; Adhi, M.; Branchini, L.; Salz, D.A.; Baumal, C.R.; Crawford, C.; Reichel, E.; Witkin, A.J.J.R. Detection of microvascular changes in eyes of patients with diabetes but not clinical diabetic retinopathy using optical coherence tomography angiography. *Retina* **2015**, *35*, 2364–2370.
66. Dimitrova, G.; Chihara, E.; Takahashi, H.; Amano, H.; Okazaki, K. Quantitative retinal optical coherence tomography angiography in patients with diabetes without diabetic retinopathy. *Investig. Ophthalmol. Vis. Sci.* **2017**, *58*, 190–196. [[CrossRef](#)] [[PubMed](#)]
67. Vujosevic, S.; Muraca, A.; Alkabes, M.; Villani, E.; Cavarzeran, F.; Rossetti, L.; De Cilla, S. Early microvascular and neural changes in patients with type 1 and type 2 diabetes mellitus without clinical signs of diabetic retinopathy. *Retina* **2019**, *39*, 435–445. [[CrossRef](#)] [[PubMed](#)]
68. Scarinci, F.; Nesper, P.L.; Fawzi, A.A. Deep retinal capillary nonperfusion is associated with photoreceptor disruption in diabetic macular ischemia. *Am. J. Ophthalmol.* **2016**, *168*, 129–138. [[CrossRef](#)] [[PubMed](#)]
69. Abcouwer, S.F.; Gardner, T.W. Diabetic retinopathy: Loss of neuroretinal adaptation to the diabetic metabolic environment. *Ann. N. Y. Acad. Sci.* **2014**, *1311*, 174–190. [[CrossRef](#)] [[PubMed](#)]
70. Zeng, Y.; Cao, D.; Yu, H.; Yang, D.; Zhuang, X.; Hu, Y.; Li, J.; Yang, J.; Wu, Q.; Liu, B. Early retinal neurovascular impairment in patients with diabetes without clinically detectable retinopathy. *Br. J. Ophthalmol.* **2019**, *103*, 1747–1752. [[PubMed](#)]
71. Rosen, R.B.; Romo, J.S.A.; Krawitz, B.D.; Mo, S.; Fawzi, A.A.; Linderman, R.; Carroll, J.; Pinhas, A.; Chui, T.Y.J. Earliest Evidence of Preclinical Diabetic Retinopathy Revealed using OCT Angiography (OCTA) Perfused Capillary Density. *Am. J. Ophthalmol.* **2019**, *203*, 103–115. [[CrossRef](#)] [[PubMed](#)]
72. Chen, Q.; Ma, Q.; Wu, C.; Tan, F.; Chen, F.; Wu, Q.; Zhou, R.; Zhuang, X.; Lu, F.; Qu, J. Macular vascular fractal dimension in the deep capillary layer as an early indicator of microvascular loss for retinopathy in type 2 diabetic patients. *Investig. Ophthalmol. Vis. Sci.* **2017**, *58*, 3785–3794. [[CrossRef](#)] [[PubMed](#)]
73. Bressler, N.M. Age-related macular degeneration is the leading cause of blindness. *JAMA* **2004**, *291*, 1900–1901. [[CrossRef](#)] [[PubMed](#)]
74. Age-Related Eye Disease Study Research Group. Risk factors associated with age-related macular degeneration: A case-control study in the age-related eye disease study: Age-related eye disease study report number 3. *Ophthalmology* **2000**, *107*, 2224–2232.
75. Spaide, R.F.; Jaffe, G.J.; Sarraf, D.; Freund, K.B.; Sadda, S.R.; Staurenghi, G.; Waheed, N.K.; Chakravarthy, U.; Rosenfeld, P.J.; Holz, F.G.; et al. Consensus nomenclature for reporting neovascular age-related macular degeneration data: Consensus on neovascular age-related macular degeneration nomenclature study group. *Ophthalmology* **2020**, *127*, 616–636. [[CrossRef](#)]
76. Freund, K.B.; Zweifel, S.A.; Engelbert, M. Do we need a new classification for choroidal neovascularization in age-related macular degeneration? *Retina* **2010**, *30*, 1333–1349. [[CrossRef](#)]
77. Gess, A.J.; Fung, A.E.; Rodriguez, J.G. Imaging in neovascular age-related macular degeneration. In *Seminars in Ophthalmology*; Taylor & Francis: Hoboken, NJ, USA, 2011; Volume 26, pp. 225–233.
78. Rosenfeld, P.J. Optical coherence tomography and the development of antiangiogenic therapies in neovascular age-related macular degeneration. *Investig. Ophthalmol. Vis. Sci.* **2016**, *57*, OCT14–OCT26. [[CrossRef](#)]
79. Palejwala, N.V.; Jia, Y.; Gao, S.S.; Liu, L.; Flaxel, C.J.; Hwang, T.S.; Lauer, A.K.; Wilson, D.J.; Huang, D.; Bailey, S.T. Detection of non-exudative choroidal neovascularization in age-related macular degeneration with optical coherence tomography angiography. *Retina* **2015**, *35*, 2204. [[CrossRef](#)]
80. Inoue, M.; Jung, J.J.; Balaratnasingam, C.; Dansingani, K.K.; Dhrami-Gavazi, E.; Suzuki, M.; Talisa, E.; Shahlaee, A.; Klufas, M.A.; El Maftouhi, A. A comparison between optical coherence tomography angiography and fluorescein angiography for the imaging of type 1 neovascularization. *Investig. Ophthalmol. Vis. Sci.* **2016**, *57*, OCT314–OCT323. [[CrossRef](#)]

81. Souied, E.H.; El Ameen, A.; Semoun, O.; Miere, A.; Querques, G.; Cohen, S.Y. Optical coherence tomography angiography of type 2 neovascularization in age-related macular degeneration. In *OCT Angiography in Retinal and Macular Diseases*; Karger Publishers: Berlin, Germany, 2016; Volume 56, pp. 52–56.
82. Kuehlewein, L.; Sadda, S.; Sarraf, D. OCT angiography and sequential quantitative analysis of type 2 neovascularization after ranibizumab therapy. *Eye* **2015**, *29*, 932. [[CrossRef](#)]
83. Coscas, G.J.; Lupidi, M.; Coscas, F.; Cagini, C.; Souied, E.H. Optical coherence tomography angiography versus traditional multimodal imaging in assessing the activity of exudative age-related macular degeneration: A new diagnostic challenge. *Retina* **2015**, *35*, 2219–2228. [[CrossRef](#)]
84. Malihi, M.; Jia, Y.; Gao, S.S.; Flaxel, C.; Lauer, A.K.; Hwang, T.; Wilson, D.J.; Huang, D.; Bailey, S.T. Optical coherence tomographic angiography of choroidal neovascularization ill-defined with fluorescein angiography. *Br. J. Ophthalmol.* **2017**, *101*, 45–50. [[CrossRef](#)]
85. Veronese, C.; Maiolo, C.; Morara, M.; Armstrong, G.W.; Ciardella, A.P. Optical coherence tomography angiography to assess pigment epithelial detachment. *Retina* **2016**, *36*, 645–650. [[CrossRef](#)]
86. Novais, E.A.; Adhi, M.; Moulton, E.M.; Louzada, R.N.; Cole, E.D.; Husvogt, L.; Lee, B.; Dang, S.; Regatieri, C.V.; Witkin, A.J. Choroidal neovascularization analyzed on ultrahigh-speed swept-source optical coherence tomography angiography compared to spectral-domain optical coherence tomography angiography. *Am. J. Ophthalmol.* **2016**, *164*, 80–88. [[CrossRef](#)]
87. Tan, A.C.; Simhaee, D.; Balaratnasingam, C.; Dansingani, K.K.; Yannuzzi, L.A. A perspective on the nature and frequency of pigment epithelial detachments. *Am. J. Ophthalmol.* **2016**, *172*, 13–27. [[CrossRef](#)] [[PubMed](#)]
88. El Ameen, A.; Cohen, S.Y.; Semoun, O.; Miere, A.; Srour, M.; Quaranta-El Maftouhi, M.; Oubraham, H.; Blanco-Garavito, R.; Querques, G.; Souied, E.H. Type 2 neovascularization secondary to age-related macular degeneration imaged by optical coherence tomography angiography. *Retina* **2015**, *35*, 2212–2218. [[CrossRef](#)] [[PubMed](#)]
89. Coscas, G.; Lupidi, M.; Coscas, F.; Français, C.; Cagini, C.; Souied, E.H. Optical coherence tomography angiography during follow-up: Qualitative and quantitative analysis of mixed type I and II choroidal neovascularization after vascular endothelial growth factor trap therapy. *Ophthalmic Res.* **2015**, *54*, 57–63. [[CrossRef](#)] [[PubMed](#)]
90. Farecki, M.L.; Gutfleisch, M.; Faatz, H.; Rothaus, K.; Heimes, B.; Spital, G.; Lommatzsch, A.; Pauleikhoff, D. Characteristics of type 1 and 2 CNV in exudative AMD in OCT-Angiography. *Graefe's Arch. Clin. Exp. Ophthalmol.* **2017**, *255*, 913–921. [[CrossRef](#)] [[PubMed](#)]
91. Schmidt-Erfurth, U.; Chong, V.; Loewenstein, A.; Larsen, M.; Souied, E.; Schlingemann, R.; Eldem, B.; Monés, J.; Richard, G.; Bandello, F. Guidelines for the management of neovascular age-related macular degeneration by the European Society of Retina Specialists (EURETINA). *Br. J. Ophthalmol.* **2014**, *98*, 1144–1167. [[CrossRef](#)] [[PubMed](#)]
92. Costanzo, E.; Miere, A.; Querques, G.; Capuano, V.; Jung, C.; Souied, E.H. Type 1 choroidal neovascularization lesion size: Indocyanine green angiography versus optical coherence tomography angiography. *Investig. Ophthalmol. Vis. Sci.* **2016**, *57*, OCT307–OCT313. [[CrossRef](#)] [[PubMed](#)]
93. Amoroso, F.; Miere, A.; Semoun, O.; Jung, C.; Capuano, V.; Souied, E.H. Optical coherence tomography angiography reproducibility of lesion size measurements in neovascular age-related macular degeneration (AMD). *Br. J. Ophthalmol.* **2018**, *102*, 821–826. [[CrossRef](#)]
94. Yanagi, Y.; Mohla, A.; Lee, W.K.; Lee, S.Y.; Mathur, R.; Chan, C.M.; Yeo, I.; Wong, T.Y.; Cheung, C.M.G. Prevalence and risk factors for nonexudative neovascularization in fellow eyes of patients with unilateral age-related macular degeneration and polypoidal choroidal vasculopathy. *Investig. Ophthalmol. Vis. Sci.* **2017**, *58*, 3488–3495. [[CrossRef](#)]
95. Roisman, L.; Zhang, Q.; Wang, R.K.; Gregori, G.; Zhang, A.; Chen, C.L.; Durbin, M.K.; An, L.; Stetson, P.F.; Robbins, G. Optical coherence tomography angiography of asymptomatic neovascularization in intermediate age-related macular degeneration. *Ophthalmology* **2016**, *123*, 1309–1319. [[CrossRef](#)]
96. De Oliveira Dias, J.R.; Zhang, Q.; Garcia, J.M.; Zheng, F.; Motulsky, E.H.; Roisman, L.; Miller, A.; Chen, C.L.; Kubach, S.; de Sistiernes, L. Natural history of subclinical neovascularization in nonexudative age-related macular degeneration using swept-source OCT angiography. *Ophthalmology* **2018**, *125*, 255–266. [[CrossRef](#)]
97. Treister, A.D.; Nesper, P.L.; Fayed, A.E.; Gill, M.K.; Mirza, R.G.; Fawzi, A.A. Prevalence of Subclinical CNV and Choriocapillaris Nonperfusion in Fellow Eyes of Unilateral Exudative AMD on OCT Angiography. *Transl. Vis. Sci. Technol.* **2018**, *7*, 19. [[CrossRef](#)] [[PubMed](#)]
98. Maguire, M.G.; Daniel, E.; Shah, A.R.; Grunwald, J.E.; Hagstrom, S.A.; Avery, R.L.; Huang, J.; Martin, R.W.; Roth, D.B.; Castellarin, A.A. Incidence of choroidal neovascularization in the fellow eye in the comparison of age-related macular degeneration treatments trials. *Ophthalmology* **2013**, *120*, 2035–2041. [[CrossRef](#)] [[PubMed](#)]
99. Pilotto, E.; Frizziero, L.; Daniele, A.R.; Convento, E.; Longhin, E.; Guidolin, F.; Parrozzani, R.; Cavarzeran, F.; Midena, E. Early OCT angiography changes of type 1 CNV in exudative AMD treated with anti-VEGF. *Br. J. Ophthalmol.* **2019**, *103*, 67–71. [[CrossRef](#)] [[PubMed](#)]
100. Bellou, S.; Pentheroudakis, G.; Murphy, C.; Fotsis, T. Anti-angiogenesis in cancer therapy: Hercules and hydra. *Cancer Lett.* **2013**, *338*, 219–228. [[CrossRef](#)] [[PubMed](#)]
101. Muakkassa, N.W.; Chin, A.T.; de Carlo, T.; Klein, K.A.; Bauman, C.R.; Witkin, A.J.; Duker, J.S.; Waheed, N.K. Characterizing the effect of anti-vascular endothelial growth factor therapy on treatment-naïve choroidal neovascularization using optical coherence tomography angiography. *Retina* **2015**, *35*, 2252–2259. [[CrossRef](#)] [[PubMed](#)]

102. Zhang, Q.; Zhang, A.; Lee, C.S.; Lee, A.Y.; Rezaei, K.A.; Roisman, L.; Miller, A.; Zheng, F.; Gregori, G.; Durbin, M.K. Projection artifact removal improves visualization and quantitation of macular neovascularization imaged by optical coherence tomography angiography. *Ophthalmol. Retin.* **2017**, *1*, 124–136. [[CrossRef](#)]
103. Spaide, R.F. Optical coherence tomography angiography signs of vascular abnormalization with antiangiogenic therapy for choroidal neovascularization. *Am. J. Ophthalmol.* **2015**, *160*, 6–16. [[CrossRef](#)]
104. Xu, J.; Song, S.; Wei, W.; Wang, R.K. Wide field and highly sensitive angiography based on optical coherence tomography with akinetic swept source. *Biomed. Opt. Express* **2017**, *8*, 420–435. [[CrossRef](#)]
105. Zhou, J.Q.; Xu, L.; Wang, S.; Wang, Y.X.; You, Q.S.; Tu, Y.; Yang, H.; Jonas, J.B. The 10-year incidence and risk factors of retinal vein occlusion: The Beijing eye study. *Ophthalmology* **2013**, *120*, 803–808. [[CrossRef](#)]
106. Tultseva, S.N.; Astakhov, Y.S.; Nechiporenko, P.A.; Ovnyanyan, A.Y.; Khatina, V.A. Ranibizumab and retinal photocoagulation in the treatment of ischemic retinal vein occlusion. *Ophthalmol. J.* **2015**, *8*, 11–27. [[CrossRef](#)]
107. Vein, T. Natural history and clinical management of central retinal vein occlusion. *Arch. Ophthalmol.* **1997**, *115*, 486–491.
108. Novais, E.A.; Waheed, N.K. Optical coherence tomography angiography of retinal vein occlusion. In *OCT Angiography in Retinal and Macular Diseases*; Karger Publishers: Berlin, Germany, 2016; Volume 56, pp. 132–138.
109. Kashani, A.H.; Lee, S.Y.; Moshfeghi, A.; Durbin, M.K.; Puliafito, C.A. Optical coherence tomography angiography of retinal venous occlusion. *Retina* **2015**, *35*, 2323–2331. [[CrossRef](#)]
110. Chung, C.Y.; Tang, H.H.Y.; Li, S.H.; Li, K.K.W. Differential microvascular assessment of retinal vein occlusion with coherence tomography angiography and fluorescein angiography: A blinded comparative study. *Int. Ophthalmol.* **2018**, *38*, 1119–1128. [[CrossRef](#)]
111. Sophie, R.; Hafiz, G.; Scott, A.W.; Zimmer-Galler, I.; Nguyen, Q.D.; Ying, H.; Do, D.V.; Solomon, S.; Sodhi, A.; Gehlbach, P. Long-term outcomes in ranibizumab-treated patients with retinal vein occlusion; the role of progression of retinal nonperfusion. *Am. J. Ophthalmol.* **2013**, *156*, 693–705.e11. [[CrossRef](#)]
112. Heier, J.S.; Campochiaro, P.A.; Yau, L.; Li, Z.; Saroj, N.; Rubio, R.G.; Lai, P. Ranibizumab for macular edema due to retinal vein occlusions: Long-term follow-up in the HORIZON trial. *Ophthalmology* **2012**, *119*, 802–809. [[CrossRef](#)]
113. Kurashige, Y.; Tsujikawa, A.; Murakami, T.; Miyamoto, K.; Ogino, K.; Muraoka, Y.; Yoshimura, N. Changes in visual acuity and foveal photoreceptor integrity in eyes with chronic cystoid macular edema associated with retinal vein occlusion. *Retina* **2012**, *32*, 792–798. [[CrossRef](#)]
114. Murakami, T.; Tsujikawa, A.; Miyamoto, K.; Sakamoto, A.; Ogino, K.; Muraoka, Y.; Kurashige, Y.; Yoshimura, N. Disrupted foveal photoreceptors after combined cystoid spaces and retinal detachment in branch vein occlusion treated with bevacizumab. *Retina* **2012**, *32*, 1853–1861. [[CrossRef](#)]
115. Wakabayashi, T.; Sato, T.; Hara-Ueno, C.; Fukushima, Y.; Sayanagi, K.; Shiraki, N.; Sawa, M.; Ikuno, Y.; Sakaguchi, H.; Nishida, K. Retinal microvasculature and visual acuity in eyes with branch retinal vein occlusion: Imaging analysis by optical coherence tomography angiography. *Investig. Ophthalmol. Vis. Sci.* **2017**, *58*, 2087–2094. [[CrossRef](#)]
116. Adhi, M.; Bonini Filho, M.A.; Louzada, R.N.; Kuehlewein, L.; Talisa, E.; Bauman, C.R.; Witkin, A.J.; Sadda, S.R.; Sarraf, D.; Reichel, E. Retinal capillary network and foveal avascular zone in eyes with vein occlusion and fellow eyes analyzed with optical coherence tomography angiography. *Investig. Ophthalmol. Vis. Sci.* **2016**, *57*, OCT486–OCT494. [[CrossRef](#)]
117. Coscas, F.; Glacet-Bernard, A.; Miere, A.; Caillaux, V.; Uzzan, J.; Lupidi, M.; Coscas, G.; Souied, E.H. Optical coherence tomography angiography in retinal vein occlusion: Evaluation of superficial and deep capillary plexa. *Am. J. Ophthalmol.* **2016**, *161*, 160–171.e2. [[CrossRef](#)]
118. Suzuki, N.; Hirano, Y.; Yoshida, M.; Tomiyasu, T.; Uemura, A.; Yasukawa, T.; Ogura, Y. Microvascular abnormalities on optical coherence tomography angiography in macular edema associated with branch retinal vein occlusion. *Am. J. Ophthalmol.* **2016**, *161*, 126–132.e1. [[CrossRef](#)] [[PubMed](#)]
119. Kang, J.W.; Yoo, R.; Jo, Y.H.; Kim, H.C. Correlation of microvascular structures on optical coherence tomography angiography with visual acuity in retinal vein occlusion. *Retina* **2017**, *37*, 1700–1709. [[CrossRef](#)] [[PubMed](#)]
120. Wang, Q.; Chan, S.Y.; Yan, Y.; Yang, J.; Zhou, W.; Jonas, J.B.; Wei, W.B. Optical coherence tomography angiography in retinal vein occlusions. *Graefes Arch. Clin. Exp. Ophthalmol.* **2018**, *256*, 1615–1622. [[CrossRef](#)] [[PubMed](#)]
121. Suzuki, N.; Hirano, Y.; Tomiyasu, T.; Esaki, Y.; Uemura, A.; Yasukawa, T.; Yoshida, M.; Ogura, Y. Retinal hemodynamics seen on optical coherence tomography angiography before and after treatment of retinal vein occlusion. *Investig. Ophthalmol. Vis. Sci.* **2016**, *57*, 5681–5687. [[CrossRef](#)]
122. Kimura, M.; Nozaki, M.; Yoshida, M.; Ogura, Y. Wide-field optical coherence tomography angiography using extended field imaging technique to evaluate the nonperfusion area in retinal vein occlusion. *Clin. Ophthalmol.* **2016**, *10*, 1291. [[CrossRef](#)]
123. Cardoso, J.N.; Keane, P.A.; Sim, D.A.; Bradley, P.; Agrawal, R.; Addison, P.K.; Egan, C.; Tufail, A. Systematic evaluation of optical coherence tomography angiography in retinal vein occlusion. *Am. J. Ophthalmol.* **2016**, *163*, 93–107.e6. [[CrossRef](#)]
124. Spaide, R.F.; Klancnik, J.M., Jr.; Cooney, M.J.; Yannuzzi, L.A.; Balaratnasingam, C.; Dansingani, K.K.; Suzuki, M. Volume-rendering optical coherence tomography angiography of macular telangiectasia type 2. *Ophthalmology* **2015**, *122*, 2261–2269. [[CrossRef](#)]
125. Salles, M.C.; Kvanta, A.; Amrén, U.; Epstein, D. Optical coherence tomography angiography in central retinal vein occlusion: Correlation between the foveal avascular zone and visual acuity. *Investig. Ophthalmol. Vis. Sci.* **2016**, *57*, OCT242–OCT246. [[CrossRef](#)]

126. Samara, W.A.; Shahlaee, A.; Sridhar, J.; Khan, M.A.; Ho, A.C.; Hsu, J. Quantitative optical coherence tomography angiography features and visual function in eyes with branch retinal vein occlusion. *Am. J. Ophthalmol.* **2016**, *166*, 76–83. [[CrossRef](#)]
127. Winegarner, A.; Wakabayashi, T.; Fukushima, Y.; Sato, T.; Hara-Ueno, C.; Busch, C.; Nishiyama, I.; Shiraki, N.; Sayanagi, K.; Nishida, K. Changes in retinal microvasculature and visual acuity after antivascular endothelial growth factor therapy in retinal vein occlusion. *Investig. Ophthalmol. Vis. Sci.* **2018**, *59*, 2708–2716. [[CrossRef](#)]
128. Ghashut, R.; Muraoka, Y.; Ooto, S.; Iida, Y.; Miwa, Y.; Suzuma, K.; Murakami, T.; Kadomoto, S.; Tsujikawa, A.; Yoshimura, N. Evaluation of macular ischemia in eyes with central retinal vein occlusion: An optical coherence tomography angiography study. *Retina* **2018**, *38*, 1571–1580. [[CrossRef](#)]
129. Shiihara, H.; Terasaki, H.; Sonoda, S.; Kakiuchi, N.; Sakamoto, T. Evaluation of Shape of Foveal Avascular Zone by Optical Coherence Tomography Angiography in Eyes With Branch Retinal Vein Occlusion. *J. Vitro. Dis.* **2018**, *2*, 138–145. [[CrossRef](#)]
130. Weinberg, D.V.; Wahle, A.E.; Ip, M.S.; Scott, I.U.; VanVeldhuisen, P.C.; Blodi, B.A.; Group, S.S.I. Score Study Report 12: Development of venous collaterals in the Score Study. *Retina* **2013**, *33*, 287. [[CrossRef](#)]
131. Falavarjani, K.G.; Phasukkijwatana, N.; Freund, K.B.; Cunningham, E.T., Jr.; Kalevar, A.; McDonald, H.R.; Dolz-Marco, R.; Roberts, P.K.; Tsui, I.; Rosen, R. En face optical coherence tomography analysis to assess the spectrum of perivenular ischemia and paracentral acute middle maculopathy in retinal vein occlusion. *Am. J. Ophthalmol.* **2017**, *177*, 131–138. [[CrossRef](#)]
132. Freund, K.B.; Sarraf, D.; Leong, B.C.; Garrity, S.T.; Vupparaboina, K.K.; Dansingani, K.K. Association of Optical Coherence Tomography Angiography of Collaterals in Retinal Vein Occlusion With Major Venous Outflow Through the Deep Vascular Complex. *Jama Ophthalmol.* **2018**, *136*, 1262–1270. [[CrossRef](#)]
133. Arrigo, A.; Carnevali, A.; Sacconi, R.; Querques, L.; Querques, G.; Bandello, F. Spontaneous retinal-choroidal anastomosis in a case of branch retinal vein occlusion. *Am. J. Ophthalmol. Case Rep.* **2018**, *11*, 92–94. [[CrossRef](#)]
134. Suzuki, N.; Hirano, Y.; Tomiyasu, T.; Kurobe, R.; Yasuda, Y.; Esaki, Y.; Yasukawa, T.; Yoshida, M.; Ogura, Y. Collateral vessels on optical coherence tomography angiography in eyes with branch retinal vein occlusion. *Br. J. Ophthalmol.* **2018**, *103*, 1373–1379. [[CrossRef](#)]
135. Campochiaro, P.A.; Brown, D.M.; Awh, C.C.; Lee, S.Y.; Gray, S.; Saroj, N.; Murahashi, W.Y.; Rubio, R.G. Sustained benefits from ranibizumab for macular edema following central retinal vein occlusion: Twelve-month outcomes of a phase III study. *Ophthalmology* **2011**, *118*, 2041–2049. [[CrossRef](#)]
136. Spaide, R.F. Volume-rendered optical coherence tomography of retinal vein occlusion pilot study. *Am. J. Ophthalmol.* **2016**, *165*, 133–144. [[CrossRef](#)]
137. Falavarjani, K.G.; Iafe, N.A.; Hubschman, J.P.; Tsui, I.; Sadda, S.R.; Sarraf, D. Optical coherence tomography angiography analysis of the foveal avascular zone and macular vessel density after anti-VEGF therapy in eyes with diabetic macular edema and retinal vein occlusion. *Investig. Ophthalmol. Vis. Sci.* **2017**, *58*, 30–34. [[CrossRef](#)]
138. Winegarner, A.; Wakabayashi, T.; Hara-Ueno, C.; Sato, T.; Busch, C.; Fukushima, Y.; Sayanagi, K.; Nishida, K.; Sakaguchi, H.; Nishida, K. Retinal microvasculature and visual acuity after intravitreal aflibercept in eyes with central retinal vein occlusion: An optical coherence tomography angiography study. *Retina* **2018**, *38*, 2067–2072. [[CrossRef](#)]
139. Hayreh, S.S. Acute retinal arterial occlusive disorders. *Prog. Retin. Eye Res.* **2011**, *30*, 359–394. [[CrossRef](#)]
140. Yu, S.; Pang, C.E.; Gong, Y.; Freund, K.B.; Yannuzzi, L.A.; Rahimy, E.; Lujan, B.J.; Tabandeh, H.; Cooney, M.J.; Sarraf, D.J. The spectrum of superficial and deep capillary ischemia in retinal artery occlusion. *Am. J. Ophthalmol.* **2015**, *159*, 53–63.e2. [[CrossRef](#)]
141. De Castro-Abeger, A.H.; de Carlo, T.E.; Duker, J.S.; Bauman, C.R. Optical coherence tomography angiography compared to fluorescein angiography in branch retinal artery occlusion. *Ophthalmic Surg. Lasers Imaging Retin.* **2015**, *46*, 1052–1054. [[CrossRef](#)]
142. Bonini Filho, M.A.; Adhi, M.; Talisa, E.; Ferrara, D.; Bauman, C.R.; Witkin, A.J.; Reichel, E.; Kuehlewein, L.; Sadda, S.R.; Sarraf, D.J.R. Optical coherence tomography angiography in retinal artery occlusion. *Retina* **2015**, *35*, 2339–2346. [[CrossRef](#)]
143. Mason, J.O., III; Patel, S.A.; Feist, R.M.; Albert, M.A., Jr.; Huisingh, C.; McGwin, G., Jr.; Thomley, M.L. Ocular neovascularization in eyes with a central retinal artery occlusion or a branch retinal artery occlusion. *Clin. Ophthalmol.* **2015**, *9*, 995. [[CrossRef](#)]
144. Bourne, R.R.; Stevens, G.A.; White, R.A.; Smith, J.L.; Flaxman, S.R.; Price, H.; Jonas, J.B.; Keeffe, J.; Leasher, J.; Naidoo, K. Causes of vision loss worldwide, 1990–2010: A systematic analysis. *Lancet Glob. Health* **2013**, *1*, e339–e349. [[CrossRef](#)]
145. Weinreb, R.N.; Khaw, P.T. Primary open-angle glaucoma. *Lancet* **2004**, *363*, 1711–1720. [[CrossRef](#)]
146. Leske, M.C.; Heijl, A.; Hyman, L.; Bengtsson, B.; Dong, L.; Yang, Z.; Group, E. Predictors of long-term progression in the early manifest glaucoma trial. *Ophthalmology* **2007**, *114*, 1965–1972. [[CrossRef](#)] [[PubMed](#)]
147. Flammer, J.; Orgül, S.; Costa, V.P.; Orzalesi, N.; Krieglstein, G.K.; Serra, L.M.; Renard, J.P.; Stefánsson, E. The impact of ocular blood flow in glaucoma. *Prog. Retin. Eye Res.* **2002**, *21*, 359–393. [[CrossRef](#)]
148. Liu, L.; Jia, Y.; Takusagawa, H.L.; Pechauer, A.D.; Edmunds, B.; Lombardi, L.; Davis, E.; Morrison, J.C.; Huang, D. Optical coherence tomography angiography of the peripapillary retina in glaucoma. *JAMA Ophthalmol.* **2015**, *133*, 1045–1052. [[CrossRef](#)] [[PubMed](#)]
149. Jia, Y.; Wei, E.; Wang, X.; Zhang, X.; Morrison, J.C.; Parikh, M.; Lombardi, L.H.; Gattley, D.M.; Armour, R.L.; Edmunds, B. Optical coherence tomography angiography of optic disc perfusion in glaucoma. *Ophthalmology* **2014**, *121*, 1322–1332. [[CrossRef](#)] [[PubMed](#)]
150. Yarmohammadi, A.; Zangwill, L.M.; Diniz-Filho, A.; Suh, M.H.; Manalastas, P.I.; Fatehee, N.; Yousefi, S.; Belghith, A.; Saunders, L.J.; Medeiros, F.A. Optical coherence tomography angiography vessel density in healthy, glaucoma suspect, and glaucoma eyes. *Investig. Ophthalmol. Vis. Sci.* **2016**, *57*, OCT451–OCT459. [[CrossRef](#)]

151. Wang, X.; Jiang, C.; Ko, T.; Kong, X.; Yu, X.; Min, W.; Shi, G.; Sun, X. Correlation between optic disc perfusion and glaucomatous severity in patients with open-angle glaucoma: An optical coherence tomography angiography study. *Graefes Arch. Clin. Exp. Ophthalmol.* **2015**, *253*, 1557–1564. [[CrossRef](#)] [[PubMed](#)]
152. Yip, V.C.; Wong, H.T.; Yong, V.K.; Lim, B.A.; Hee, O.K.; Cheng, J.; Fu, H.; Lim, C.; Tay, E.L.; Loo-Valdez, R.G. Optical Coherence Tomography Angiography of Optic Disc and Macula Vessel Density in Glaucoma and Healthy Eyes. *J. Glaucoma* **2019**, *28*, 80–87. [[CrossRef](#)] [[PubMed](#)]
153. Moghimi, S.; Zangwill, L.M.; Penteado, R.C.; Hasenstab, K.; Ghahari, E.; Hou, H.; Christopher, M.; Yarmohammadi, A.; Manalastas, P.I.C.; Shoji, T. Macular and optic nerve head vessel density and progressive retinal nerve fiber layer loss in glaucoma. *Ophthalmology* **2018**, *125*, 1720–1728. [[CrossRef](#)] [[PubMed](#)]
154. Yarmohammadi, A.; Zangwill, L.M.; Diniz-Filho, A.; Suh, M.H.; Yousefi, S.; Saunders, L.J.; Belghith, A.; Manalastas, P.I.C.; Medeiros, F.A.; Weinreb, R.N. Relationship between optical coherence tomography angiography vessel density and severity of visual field loss in glaucoma. *Ophthalmology* **2016**, *123*, 2498–2508. [[CrossRef](#)]
155. Mammo, Z.; Heisler, M.; Balaratnasingam, C.; Lee, S.; Yu, D.Y.; Mackenzie, P.; Schendel, S.; Merkur, A.; Kirker, A.; Albiani, D. Quantitative optical coherence tomography angiography of radial peripapillary capillaries in glaucoma, glaucoma suspect, and normal eyes. *Am. J. Ophthalmol.* **2016**, *170*, 41–49. [[CrossRef](#)]
156. Akagi, T.; Iida, Y.; Nakanishi, H.; Terada, N.; Morooka, S.; Yamada, H.; Hasegawa, T.; Yokota, S.; Yoshikawa, M.; Yoshimura, N. Microvascular density in glaucomatous eyes with hemifield visual field defects: An optical coherence tomography angiography study. *Am. J. Ophthalmol.* **2016**, *168*, 237–249. [[CrossRef](#)]
157. Suwan, Y.; Geyman, L.S.; Fard, M.A.; Tantraworasin, A.; Chui, T.Y.; Rosen, R.B.; Ritch, R. Peripapillary Perfused Capillary Density in Exfoliation Syndrome and Exfoliation Glaucoma versus POAG and Healthy Controls: An OCTA Study. *Asia-Pac. J. Ophthalmol.* **2018**, *7*, 84–89.
158. Sripsema, N.K.; Garcia, P.M.; Bavier, R.D.; Chui, T.Y.; Krawitz, B.D.; Mo, S.; Agemy, S.A.; Xu, L.; Lin, Y.B.; Panarelli, J.F. Optical coherence tomography angiography analysis of perfused peripapillary capillaries in primary open-angle glaucoma and normal-tension glaucoma. *Investig. Ophthalmol. Vis. Sci.* **2016**, *57*, OCT611–OCT620. [[CrossRef](#)]
159. Suh, M.H.; Zangwill, L.M.; Manalastas, P.I.C.; Belghith, A.; Yarmohammadi, A.; Medeiros, F.A.; Diniz-Filho, A.; Saunders, L.J.; Yousefi, S.; Weinreb, R.N. Optical coherence tomography angiography vessel density in glaucomatous eyes with focal lamina cribrosa defects. *Ophthalmology* **2016**, *123*, 2309–2317. [[CrossRef](#)]
160. Yarmohammadi, A.; Zangwill, L.M.; Diniz-Filho, A.; Saunders, L.J.; Suh, M.H.; Wu, Z.; Manalastas, P.I.C.; Akagi, T.; Medeiros, F.A.; Weinreb, R.N. Peripapillary and macular vessel density in patients with glaucoma and single-hemifield visual field defect. *Ophthalmology* **2017**, *124*, 709–719. [[CrossRef](#)]
161. Shoji, T.; Zangwill, L.M.; Akagi, T.; Saunders, L.J.; Yarmohammadi, A.; Manalastas, P.I.C.; Penteado, R.C.; Weinreb, R.N. Progressive macula vessel density loss in primary open-angle glaucoma: A longitudinal study. *Am. J. Ophthalmol.* **2017**, *182*, 107–117. [[CrossRef](#)]
162. Takusagawa, H.L.; Liu, L.; Ma, K.N.; Jia, Y.; Gao, S.S.; Zhang, M.; Edmunds, B.; Parikh, M.; Tehrani, S.; Morrison, J.C. Projection-resolved optical coherence tomography angiography of macular retinal circulation in glaucoma. *Ophthalmology* **2017**, *124*, 1589–1599. [[CrossRef](#)]
163. Akil, H.; Huang, A.S.; Francis, B.A.; Sadda, S.R.; Chopra, V. Retinal vessel density from optical coherence tomography angiography to differentiate early glaucoma, pre-perimetric glaucoma and normal eyes. *PLoS ONE* **2017**, *12*, e0170476. [[CrossRef](#)]
164. Rao, H.L.; Pradhan, Z.S.; Weinreb, R.N.; Reddy, H.B.; Riyazuddin, M.; Dasari, S.; Palakurthy, M.; Puttaiah, N.K.; Rao, D.A.; Webers, C.A. Regional comparisons of optical coherence tomography angiography vessel density in primary open-angle glaucoma. *Am. J. Ophthalmol.* **2016**, *171*, 75–83. [[CrossRef](#)]
165. Venugopal, J.P.; Rao, H.L.; Weinreb, R.N.; Pradhan, Z.S.; Dasari, S.; Riyazuddin, M.; Puttaiah, N.K.; Rao, D.A.; Devi, S.; Mansouri, K. Repeatability of vessel density measurements of optical coherence tomography angiography in normal and glaucoma eyes. *Br. J. Ophthalmol.* **2018**, *102*, 352–357. [[CrossRef](#)]
166. Rao, H.L.; Sreenivasiah, S.; Dixit, S.; Riyazuddin, M.; Dasari, S.; Venugopal, J.P.; Pradhan, Z.S.; Puttaiah, N.K.; Devi, S.; Mansouri, K. Choroidal Microvascular Dropout in Primary Open-angle Glaucoma Eyes with Disc Hemorrhage. *J. Glaucoma* **2018**, *28*, 181–187. [[CrossRef](#)]
167. Jung, J.H.; Park, J.H.; Yoo, C.; Kim, Y.Y. Localized retinal nerve fiber layer defects in red-free photographs versus en face structural optical coherence tomography images. *J. Glaucoma* **2018**, *27*, 269–274. [[CrossRef](#)]
168. Hayreh, S. Ischaemic optic neuropathy. *Indian J. Ophthalmol.* **2000**, *48*, 171. [[PubMed](#)]
169. Arnold, A.C. The 14th Hoyt Lecture: Ischemic Optic Neuropathy The Evolving Profile, 1966–2015. *J. Neuro-Ophthalmol.* **2016**, *36*, 208–215. [[CrossRef](#)] [[PubMed](#)]
170. Hayreh, S.S. Management of ischemic optic neuropathies. *Indian J. Ophthalmol.* **2011**, *59*, 123. [[CrossRef](#)] [[PubMed](#)]
171. Cestari, D.M.; Gaier, E.D.; Bouzika, P.; Blachley, T.S.; De Lott, L.B.; Rizzo, J.F.; Wiggs, J.L.; Kang, J.H.; Pasquale, L.R.; Stein, J.D. Demographic, systemic, and ocular factors associated with nonarteritic anterior ischemic optic neuropathy. *Ophthalmology* **2016**, *123*, 2446–2455. [[CrossRef](#)]
172. Balducci, N.; Morara, M.; Veronese, C.; Barboni, P.; Casadei, N.L.; Savini, G.; Parisi, V.; Sadun, A.A.; Ciardella, A. Optical coherence tomography angiography in acute arteritic and non-arteritic anterior ischemic optic neuropathy. *Graefes Arch. Clin. Exp. Ophthalmol.* **2017**, *255*, 2255–2261. [[CrossRef](#)]

173. Ling, J.W.; Yin, X.; Lu, Q.Y.; Chen, Y.Y.; Lu, P.R. Optical coherence tomography angiography of optic disc perfusion in non-arteritic anterior ischemic optic neuropathy. *Int. J. Ophthalmol.* **2017**, *10*, 1402.
174. Song, Y.; Min, J.; Mao, L.; Gong, Y. Microvasculature dropout detected by the optical coherence tomography angiography in nonarteritic anterior ischemic optic neuropathy. *Lasers Surg. Med.* **2018**, *50*, 194–201. [[CrossRef](#)]
175. Mayes, E.W.; Cole, E.D.; Dang, S.; Novais, E.A.; Vuong, L.; Mendoza-Santiesteban, C.; Duker, J.S.; Hedges, T.R., III. Optical coherence tomography angiography in nonarteritic anterior ischemic optic neuropathy. *J. Neuro-Ophthalmol.* **2017**, *37*, 358–364. [[CrossRef](#)]
176. Augstburger, E.; Zéboulon, P.; Keilani, C.; Baudouin, C.; Labbé, A. Retinal and choroidal microvasculature in nonarteritic anterior ischemic optic neuropathy: An optical coherence tomography angiography study. *Investig. Ophthalmol. Vis. Sci.* **2018**, *59*, 870–877. [[CrossRef](#)]
177. Sharma, S.; Ang, M.; Najjar, R.P.; Sng, C.; Cheung, C.Y.; Rukmini, A.V.; Schmetterer, L.; Milea, D. Optical coherence tomography angiography in acute non-arteritic anterior ischaemic optic neuropathy. *Br. J. Ophthalmol.* **2017**, *101*, 1045–1051. [[CrossRef](#)]
178. Mase, T.; Ishibazawa, A.; Nagaoka, T.; Yokota, H.; Yoshida, A. Radial peripapillary capillary network visualized using wide-field montage optical coherence tomography angiography. *Investig. Ophthalmol. Vis. Sci.* **2016**, *57*, OCT504–OCT510. [[CrossRef](#)]
179. You, Q.S.; Guo, Y.; Wang, J.; Wei, X.; Camino, A.; Zang, P.; Flaxel, C.J.; Bailey, S.T.; Huang, D.; Jia, Y.; et al. Detection of clinically unsuspected retinal neovascularization with wide-field optical coherence tomography angiography. *Retina* **2019**, *40*, 891–897. [[CrossRef](#)]
180. Zhang, Q.; Lee, C.S.; Chao, J.; Chen, C.L.; Zhang, T.; Sharma, U.; Zhang, A.; Liu, J.; Rezaei, K.; Pepple, K.L. Wide-field optical coherence tomography based microangiography for retinal imaging. *Sci. Rep.* **2016**, *6*, 22017. [[CrossRef](#)]
181. Hirano, T.; Kakihara, S.; Toriyama, Y.; Nittala, M.G.; Murata, T.; Sadda, S. Wide-field en face swept-source optical coherence tomography angiography using extended field imaging in diabetic retinopathy. *Br. J. Ophthalmol.* **2018**, *102*, 1199–1203. [[CrossRef](#)]
182. Jia, Y.; Tan, O.; Tokayer, J.; Potsaid, B.; Wang, Y.; Liu, J.J.; Kraus, M.F.; Subhash, H.; Fujimoto, J.G.; Hornegger, J. Split-spectrum amplitude-decorrelation angiography with optical coherence tomography. *Opt. Express* **2012**, *20*, 4710–4725. [[CrossRef](#)]
183. Falavarjani, K.G.; Al-Sheikh, M.; Akil, H.; Sadda, S.R. Image artefacts in swept-source optical coherence tomography angiography. *Br. J. Ophthalmol.* **2017**, *101*, 564–568. [[CrossRef](#)]
184. Spaide, R.F.; Fujimoto, J.G.; Waheed, N.K. Image artifacts in optical coherence angiography. *Retina* **2015**, *35*, 2163. [[CrossRef](#)]
185. Camino, A.; Zhang, M.; Gao, S.S.; Hwang, T.S.; Sharma, U.; Wilson, D.J.; Huang, D.; Jia, Y. Evaluation of artifact reduction in optical coherence tomography angiography with real-time tracking and motion correction technology. *Biomed. Opt. Express* **2016**, *7*, 3905–3915. [[CrossRef](#)]
186. Akil, H.; Falavarjani, K.G.; Sadda, S.R.; Sadun, A.A. Optical coherence tomography angiography of the optic disc: An overview. *J. Ophthalmic Vis. Res.* **2017**, *12*, 98.